

# LOGICS-PARSING-OMNI TECHNICAL REPORT

Logics Team

Alibaba Group

(For the complete list of authors, please refer to the Contribution section)

## ABSTRACT

Addressing the challenges of fragmented task definitions and the heterogeneity of unstructured data in multimodal parsing, this paper proposes the Omni Parsing framework. This framework establishes a Unified Taxonomy covering documents, images, and audio-visual streams, introducing a progressive parsing paradigm that bridges perception and cognition. Specifically, the framework integrates three hierarchical levels: 1) Holistic Detection, which achieves precise spatial-temporal grounding of objects or events to establish a geometric baseline for perception; 2) Fine-grained Recognition, which performs symbolization (e.g., OCR/ASR) and attribute extraction on localized objects to complete structured entity parsing; and 3) Multi-level Interpreting, which constructs a reasoning chain from local semantics to global logic. A pivotal advantage of this framework is its evidence anchoring mechanism, which enforces a strict alignment between high-level semantic descriptions and low-level facts. This enables “evidence-based” logical induction, transforming unstructured signals into standardized knowledge that is locatable, enumerable, and traceable. Building on this foundation, we constructed a standardized dataset and released the Logics-Parsing-Omni model, which successfully converts complex audio-visual signals into machine-readable structured knowledge. Experiments demonstrate that fine-grained perception and high-level cognition are synergistic, effectively enhancing model reliability. Furthermore, to quantitatively evaluate these capabilities, we introduce OmniParsingBench. Code, models and the benchmark are released at <https://github.com/alibaba/Logics-Parsing/tree/master/Logics-Parsing-Omni>.

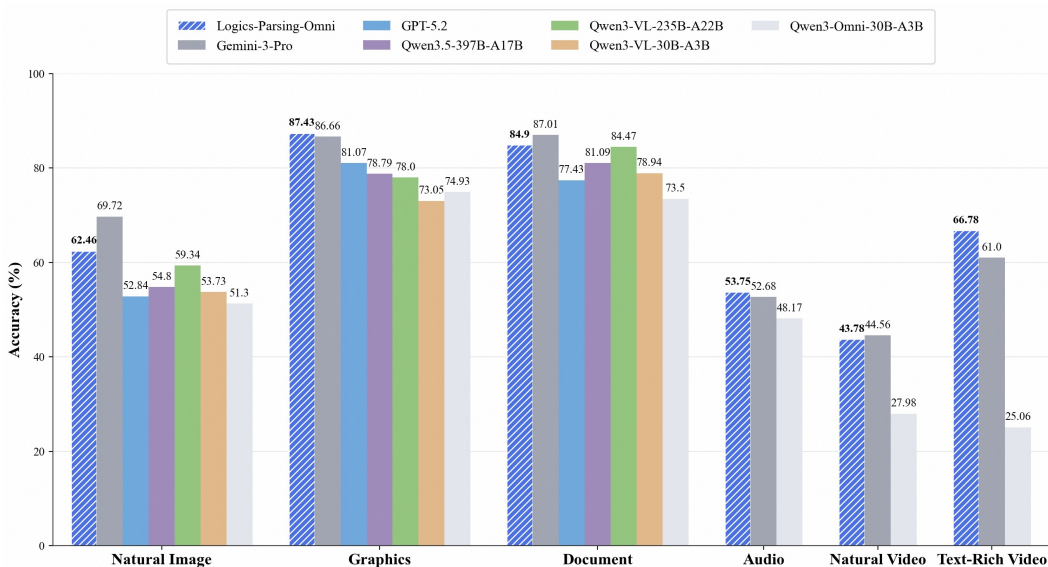


Figure 1: OmniParsingBench performance of Logics-Parsing-Omni.

arXiv:2603.09677v1 [cs.AI] 10 Mar 2026

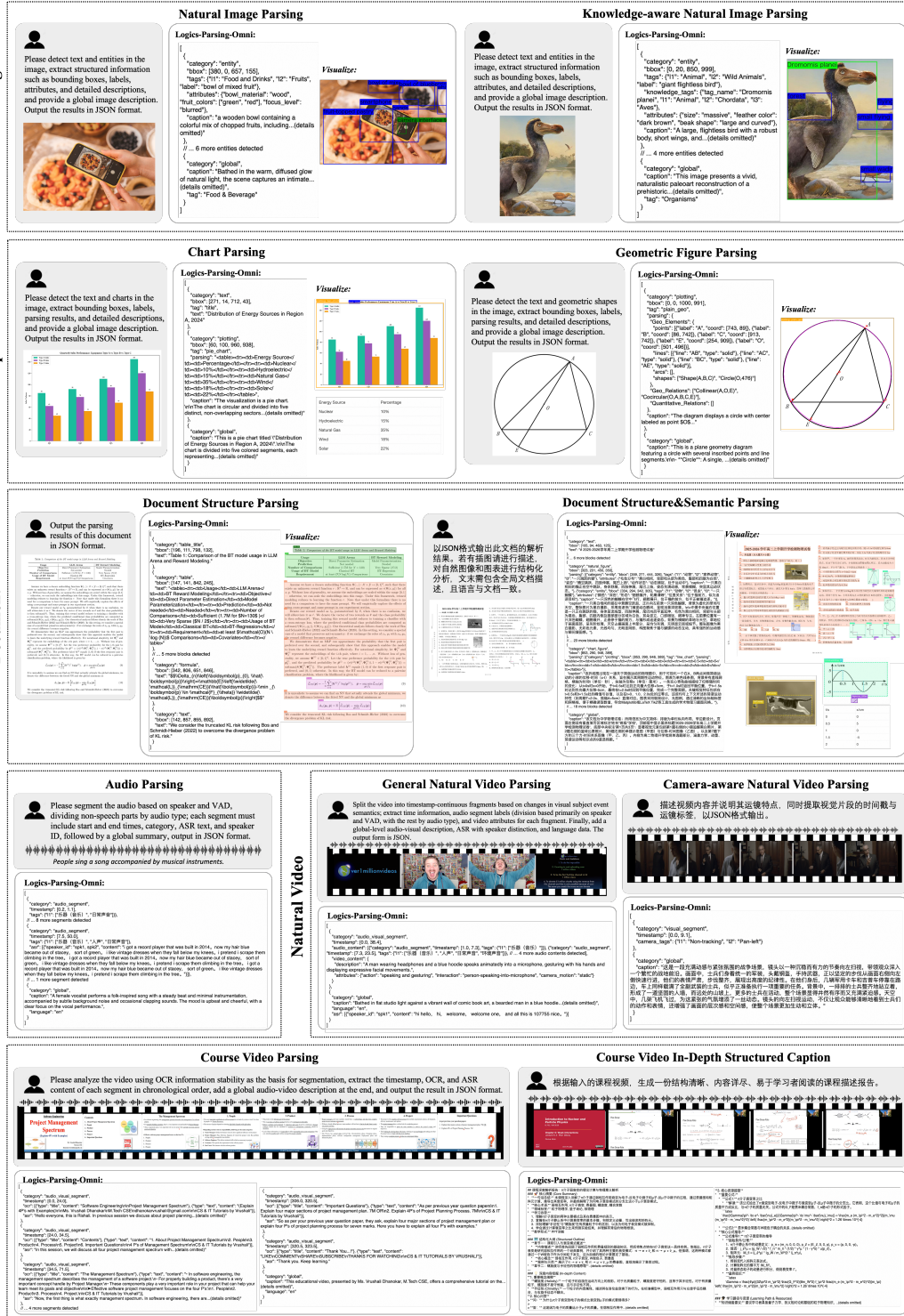


Figure 2: Showcase of the multifaceted capabilities of Logics-Parsing-Omni.

# 1 INTRODUCTION

In recent years, Multimodal Large Language Models (MLLMs) have demonstrated remarkable general-purpose capabilities Liu et al. (2023); An et al. (2025); Bai et al. (2025a); Yang et al.

---

(2025). However, applying them to knowledge-intensive domains remains challenging, particularly in visual-rich documents and long-form educational videos. These media feature high-density text, complex layouts, and diverse non-text visual content (e.g., illustrations, charts, and slides). For practical deployment, neither low-level extraction (e.g., OCR or layout analysis) nor free-form high-level semantic descriptions alone are sufficient. An effective system requires the integration of fine-grained content parsing with deep semantic understanding to produce a unified representation that is locatable, indexable, and summarizable—thereby enabling robust downstream tasks such as Retrieval-Augmented Generation (RAG), Question Answering (QA), and intelligent tutoring.

Current approaches face structural dilemmas across modalities. In the document domain, traditional pipelines Wei et al. (2024); Poznanski et al. (2025); Cui et al. (2025c) excel at layout analysis but often reduce complex figures and charts to mere bounding boxes, stripping them of semantic value. This leads to the loss of critical information such as trends, comparisons, causal relations, and chart insights, rendering them unusable for deep retrieval. While LLM-based approaches Wang et al. (2024b); Bai et al. (2025b) generate fluent descriptions, they often lack layout fidelity and fine-grained grounding, limiting their utility in automated document conversion and indexing pipelines. Similarly, in image understanding, generalist models often fail to capture the dense, attribute-rich information (e.g., specific chart data or spatial relations) required for complex reasoning and tend to hallucinate or gloss over these details in favor of generic descriptions. The audio-visual domain faces even greater hurdles: relying solely on linear ASR transcripts overlooks non-speech acoustic events (e.g., background noises, emotional cues) and visual contexts (e.g., slides), while generic video captions Xu et al. (2025a;b); AI et al. (2025); Team et al. (2025b) lack the structural granularity to organize long-form content. Consequently, there is a critical need for a system that unifies reliable, fine-grained parsing with application-oriented semantic understanding.

To this end, we propose the Omni Parsing framework, establishing a unified parsing taxonomy across documents, images, and audio-visual streams. Unlike traditional paradigms treating perception and cognition separately, Omni Parsing introduces a progressive paradigm to bridge pixel-based perception and logic-based cognition. We define “Omni Parsing” as transforming unstructured signals into standardized knowledge that is Locatable, Enumerable, and Traceable. This ensures that the understanding of visual elements—whether document diagrams or video events—is not merely descriptive but forms an indispensable part of a structured, fact-based reasoning chain.

Building on this framework, we release Logics-Parsing-Omni, an advanced MLLM designed to instantiate this progressive parsing paradigm across all modalities. The model is optimized for three synergistic tasks: Holistic Detection for spatiotemporal localization; Fine-grained Recognition for symbol and attribute extraction; and Semantic Interpretation for logical reasoning. Crucially, the model’s performance is driven by a data-centric strategy. We significantly enriched knowledge-intensive image samples to enhance entity-rich reasoning. Furthermore, for the video domain, we specifically optimized annotations for fine-grained shot analysis and long educational content, ensuring accurate temporal localization and narrative understanding. This approach effectively anchors generation in facts, resulting in semantically rich and verifiable outputs. To provide a quantitative overview of omni-modal parsing, we built an internal OmniParsingBench covering document, image, and audio-video content. Figure 1 compares Logics-Parsing-Omni with representative baseline models on OmniParsingBench. The results show consistent improvements across all modalities, demonstrating that the model maintains a strong balance between structural fidelity and semantic interpretation. Beyond quantitative results, Figure 2 provides a compact qualitative showcase of our unified parsing across modalities.

The main contributions of our work can be summarized as follows:

- **Unified Framework:** We propose the Omni Parsing framework, defining a three-level progressive paradigm—integrating Holistic Detection, Fine-grained Recognition, and Semantic Interpretation—to unify perception and cognition across documents, images, and audio-visual streams.
- **Data & Methodology:** We constructed a standardized, high-quality dataset tailored for omni-modal parsing. By integrating knowledge-intensive image data and optimizing video annotations for structural analysis, we enable the model to master both complex static entities and dynamic narrative logic.
- **Model & Benchmark:** We release Logics-Parsing-Omni, a model capable of converting complex multimodal signals into machine-readable knowledge, and open-source OmniParsingBench

to facilitate the quantitative evaluation of fine-grained parsing capabilities, providing robust infrastructure for the community.

## 2 METHODOLOGY

In this section, we present the methodology of Logics-Parsing-Omni. Leveraging data structured by our three-level progressive parsing framework, we employ a two-stage training paradigm designed to seamlessly connect fine-grained perception with high-level cognition. We first introduce the overall framework (Section 2.1), then describe the construction of training data (Section 2.2), and finally detail the training procedure (Section 2.3).

### 2.1 OVERVIEW

As illustrated in Figure 3, the foundation of our approach is the construction of a large-scale unified corpus that systematically integrates heterogeneous tasks across four core modalities: Document, Image, Audio, and Video. Rather than treating these modalities in isolation, we unify diverse objectives—ranging from structural and semantic parsing in documents, to single and multi-image difference analysis (across natural scenes and graphics), as well as complex temporal understanding in diverse audio and video environments. By formulating these multifaceted tasks into a cohesive data pipeline, we encourage the model to jointly learn localized structural fidelity and high-level semantic logic.

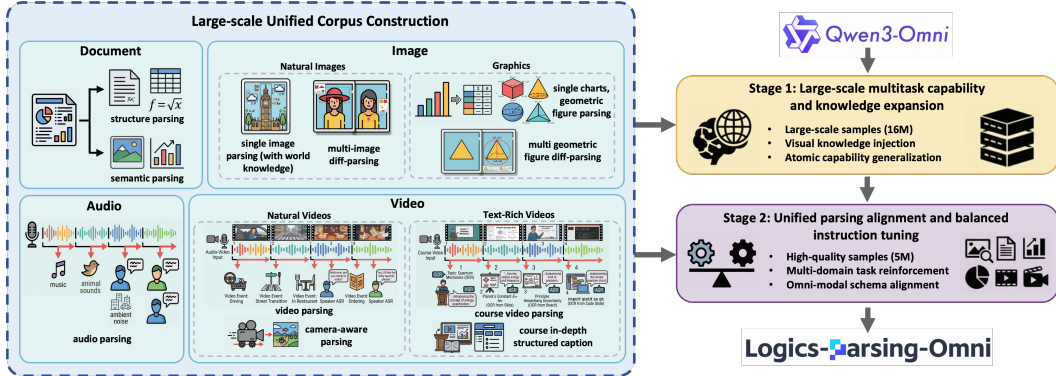


Figure 3: The construction of unified multi-modal parsing corpus and training pipeline of our proposed Logics-Parsing-Omni.

We adopt a two-stage progressive training strategy. The first stage, Panoramic Cognitive Foundation, prioritizes data scale and coverage to foster broad visual knowledge and atomic capabilities. Through exposure to diverse multi-source tasks, the model masters pure structural parsing and isolated semantic recognition without being overwhelmed by complex reasoning. Building upon this, the second stage, Unified Parsing Alignment, refines the model using high-quality, balanced instructions. This progression ensures the model maps heterogeneous omni-modal inputs into standardized JSON formats while preserving fluent natural language generation, achieving a deep integration of perception and cognition.

### 2.2 DATASET

As illustrated in Figure 4, we construct a large-scale, diverse, and high-quality corpus for unified parsing across modalities. To support the progressive training strategy in Section 2.1 — including both layout-faithful structural parsing and semantic interpretation of visual elements, the corpus covers four domains: Image, Document, Audio and Video:

- **Image.** This domain encompasses both natural images and information-centric graphics (e.g., charts and geometric figures). It explicitly transforms visual content into standardized, machine-readable formats with precise spatial localization, fine-grained semantic interpretation, and reliable knowledge association.

- **Document.** We adopt a unified schema for the layout-faithful extraction of heterogeneous elements, including text, tables, and mathematical formulas. Crucially, it moves beyond traditional OCR by contextually interpreting embedded visual elements (e.g., illustrations) into searchable semantic descriptions, ensuring comprehensive document understanding.
- **Audio.** Moving beyond treating audio merely as a source of speech, we decode it as a multi-dimensional sensory channel. This domain provides precise, time-aligned semantic chunks that seamlessly integrate speaker-attributed transcriptions with fine-grained acoustic events and overarching scene descriptions.
- **Video.** Extending spatial parsing into the temporal dimension, this domain hierarchically fuses visual dynamics, audio signals, and explicit camera motion. It also encompasses text-rich instructional videos, effectively converting complex, long-form audio-visual streams into temporally aligned, structured multimodal knowledge.

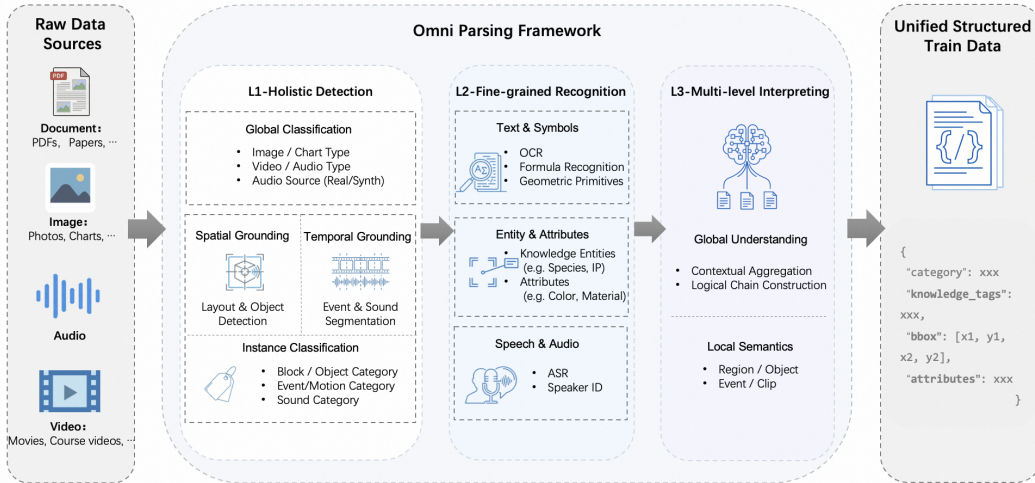


Figure 4: Overview of the Omni Parsing Framework. The framework transforms multimodal raw data into unified structured training data via three progressive stages: (1) L1-Holistic Detection: Performs spatio-temporal grounding and coarse classification; (2) L2-Fine-grained Recognition: Extracts detailed text, symbols, knowledge, attributes, and speech content; (3) L3-Multi-level Interpreting: Synthesizes local semantics with global logical reasoning. The final output is a standardized JSON format containing all parsing results from L1 to L3.

The detailed statistics are summarized in Table 1. The corpus is constructed as a hybrid mixture across all four modalities: it includes not only the unified structured parsing data generated by our Omni Parsing framework, but also diverse Caption and QA data. This specific data composition directly fuels our two-stage training strategy. It provides the 16M large-scale knowledge coverage necessary to establish atomic capabilities and basic perception in Stage 1, while offering the 5M high-precision instructional support required for deep balanced fine-tuning and complex reasoning in Stage 2. Ultimately, this ensures the model achieves consistent full-modal alignment from basic structure to advanced semantics.

### 2.2.1 IMAGE

**Natural Images.** To address the limitations of traditional captioning, such as subjective ambiguity, absence of spatial localization, coarse semantic granularity, and unstructured expression, we propose a structured parsing approach that deconstructs images into a standardized JSON format.

- **Single-Image.** This module transforms visual content into logically coherent, machine-friendly structured data. By explicitly anchoring semantics to spatial regions while preserving readability, it significantly enhances utility in fine-grained retrieval, cross-modal alignment, and accessibility services.
  - **Parsing Format:** The output follows a unified schema comprising three structured components: Entity Objects (encapsulating attributes, normalized coordinates, and objective descrip-

Table 1: Detailed statistics of the constructed corpus.

Domain	Data Category	Task	# Samples	
Document	General Document	Parsing (Structure)	342K	
		Parsing (Structure&Semantic)	333K	
Image	Natural Image	Caption (Single-Image)	360K	
		Parsing (Single-Image)	411K	
		Caption (Diff, Multi-Image)	354K	
		Parsing (Diff, Multi-Image)	212K	
	Knowledge-aware Natural Image	QA	12.6M	
		Caption	400K	
		Parsing	400K	
	Graphics		Charts Caption	132K
			Charts Parsing	176K
			Geometric Caption (Single-Image)	266K
Geometric Parsing (Single-Image)			174K	
Geometric Caption (Diff, Multi-Image)			444K	
Geometric Parsing (Diff, Multi-Image)			358K	
Audio	General Audio	QA	100K	
		Caption	511K	
		Parsing	266K	
Video	General Natural Video	QA	30K	
		Caption	620K	
		Parsing	269K	
	Camera-aware Natural Video	QA	97K	
		Caption	47K	
		Parsing	47K	
	Text-Rich Video		Caption (General)	90K
			Caption (In-Depth)	130K
			Parsing	79K

tions), Text Blocks (preserving layout, functional categories, and multilingual transcriptions), and Global Descriptions (integrating scene classification with a cohesive spatial narrative). This standardized format ensures all visual elements are locatable and interpretable, facilitating flexible integration into downstream tasks.

- **Knowledge-aware Entity Parsing:** To bridge the gap between generic descriptions and specific identities, we introduce a strict Knowledge Enhancement Mechanism. Entities are linked to authoritative identifiers (e.g., landmarks, brands, species) solely when visual evidence is unambiguous. By integrating these verified knowledge tags into the narrative, we transform unstructured signals into precise, actionable knowledge, essential for applications like semantic search.
- **Data Preparation:** The dataset is constructed via a collaborative pipeline combining expert model synthesis (Detection, OCR) with rule-based standardization. Knowledge tags are injected exclusively for validated entities, while global descriptions are refined by an LLM that synthesizes multi-perspective drafts into a coherent narrative. The final corpus undergoes automated validation to ensure high quality.
- **Multi-Image.** To enhance the model’s capability in recognizing fine-grained differences in natural images, we constructed a high-quality Image Difference Dataset. We formed image pairs from real-world collections, applying rigorous VLM-based filtering to ensure consistency and aesthetic quality. The annotation process employs a fully automated closed-loop pipeline: a VLM first analyzes semantic discrepancies to generate descriptive captions, which then prompt a Grounding

---

VLM to precisely localize differing regions. This ensures strict alignment between linguistic descriptions and geometric grounding. By leveraging real-world imagery rather than synthetic artifacts, our dataset provides high-fidelity supervision for fine-grained visual comparison tasks, establishing a reliable benchmark for training and evaluating models.

**Graphics.** To enhance the model’s capability in accurately interpreting and reasoning over information-dense visual elements, we curated a specialized structural repository focusing on charts and geometric figures.

- **Charts.** We integrated diverse chart samples from multiple public datasets Li et al. (2024); Hu et al. (2024); Deka (2025); Roecker (2024); LLM (2025); tbt0205 (2025) (e.g., line/bar/pie charts, flowcharts, infographics). To align with the Omni Parsing framework, we annotated these data following our three-level progressive paradigm: In the *L1 & L2 stages (Detection & Recognition)*, we decouple plotting regions from auxiliary text regions. Texts are extracted and classified by functional tags (e.g., titles), while plotting regions undergo fine-grained categorization to ensure all visual entities are locatable. In the *L3 stage (Semantic Interpreting)*, we utilize Qwen3-VL-235B-A22B-Instruct to reverse-engineer visual elements into precise structured formats. Specifically, statistical charts are parsed into HTML tables (`<table> . . . </table>`), while flowcharts and relational diagrams are transcribed into Mermaid code. This ensures high-precision extraction of data series and aligns perfectly with table parsing in the Document domain. Based on this, we generate *Local Captions* detailing chart types, axes, legends, and specific data points, followed by a *Global Caption* that explicitly interprets overarching data trends, distributions, and key annotations.
- **Geometric Figures.** To tackle the complex spatial topology and mathematical constraints of geometric figures, we construct two subsets covering single-image interpretation and multi-image difference parsing:
  - **Single-Image.** Sourced from K–12 textbooks and public datasets Li et al. (2024); Peng et al. (2024), we decouple plotting regions from textual contexts (e.g., mathematical problem stems). We synthesize structured data encapsulating three dimensions: *Geometric Elements* (precise localization of points/lines/polygons), *Topological Relations* (e.g., parallelism), and *Quantitative Relations* (e.g., lengths/radii). For plane geometry, the overarching logic is synthesized via Qwen3-VL-235B-A22B-Thinking, with coordinates and radii anchored by a specialized recognition model. Due to severe viewpoint complexities, 3D solid geometry is parsed using Gemini-3-Pro. Finally, we generate *Local Captions* detailing primitives and metric annotations, and *Global Captions* fusing visual logic with the textual context.
  - **Multi-Image.** We construct minimal-edit image pairs differing by only atomic operations (e.g., drawing an angle bisector). To enable fine-grained reasoning, annotations are structured into two levels: the *Plotting level* specifies differential visual elements (added primitives, coordinates) and constraints (geometric/quantitative), while the *Global level* provides natural-language editing instructions. The English subset is synthesized via an enhanced MathCanvas pipeline, and the Chinese subset is mined from K–12 textbooks using Qwen3-VL. All candidate pairs are rigorously filtered to ensure semantically meaningful and curriculum-aligned transformations.

## 2.2.2 DOCUMENT

For the document parsing task, we choose to leverage the supervised fine-tuning (SFT) dataset originally introduced in our prior *Logics-Parsing* Chen et al. (2025) framework. Empirical evaluations have demonstrated that this dataset effectively equips the *Logics-Parsing* model with robust document parsing capabilities, attributed to its comprehensive coverage of heterogeneous document types as well as balanced distribution of English and Chinese content. Concretely, the dataset is constructed from two complementary sources. The first comprises data aggregated from several well-established public datasets, whose original annotations are normalized into a unified JSON annotation schema, including olmOCR-mix-0225 Poznanski et al. (2025) for page-level parsing, FinTabNet Zheng et al. (2020), TNCr Abdallah et al. (2021), and PubTabNet Zhong et al. (2019) for table recognition sub-task, as well as ChEBI-20-MM dataset Liu et al. (2025a) for chemical structure recognition. The second source originates from a large-scale in-house dataset processed through a rigorous two-stage annotation pipeline which involves automated pre-annotation and ex-

---

pert refinement (both model-assisted and human-verified). In total, more than 300K high-quality page-level document images are collected for document parsing task.

Beyond traditional OCR and layout analysis, we explicitly integrate fine-grained structured parsing for embedded non-text elements (e.g., illustrations, charts). This unified modeling captures text-vision logical connections, unlocking the semantic value of figures for deep retrieval.

### 2.2.3 AUDIO

To decode the multifaceted signals within the audio modality, we construct a time-aligned parsing process that integrates non-dialogue acoustic events with speaker identification to support high-fidelity cross-modal inference.

- **Speaker-Attributed Transcription.** Utilizing the CAM++ Wang et al. (2023) model, we perform speaker diarization to assign unique speaker IDs to distinct audio segments. These segments are transcribed using FireRedASR Xu et al. (2025c) and Whisper Radford et al. (2022), establishing a synchronized "SpeakerID-ASR-Timestamp" triplet. This ensures that every utterance is precisely anchored to a specific identity and time interval.
- **Acoustic Scene Modeling.** To capture non-linguistic cues, we employ the DASM Cai et al. (2025) framework for dense acoustic event detection. DASM identifies over 500 granular acoustic classes, which we distill into six macro-categories: Human Voice, Instrumental Music, Environmental Noise, Traffic, Animals, and Daily Life Sounds. We optimize classification thresholds to generate high-precision, timestamped acoustic labels.
- **Unified Audio Semantic Chunks.** We synthesize these streams by using speaker segments as the primary temporal units, overlaying DASM-detected acoustic events while merging overlapping intervals and removing noise. The resulting Audio Semantic Chunks contain start/end boundaries, Speaker IDs, ASR text, and acoustic event tags, complemented by holistic scene descriptions from MidasHengLM Horizon Team, MiLM Plus (2025).

This design ensures that audio is no longer treated merely as a text source but as a multi-dimensional channel carrying identity and environmental context, providing high-resolution supervision for cross-modal alignment.

### 2.2.4 VIDEO

**Natural Videos.** Existing video parsing systems often exhibit two major blind spots: they underutilize the audio modality (treating it merely as ASR transcripts and ignoring acoustic cues or speaker identity) and they overlook fine-grained camera motion, which is critical for directing attention, shaping narrative rhythm, and conveying emotion. To address these limitations and capture holistic scene dynamics, we curate two natural video datasets: General Video and Camera-aware Video.

- **General Video.** To resolve cross-modal inconsistencies and fully exploit non-linguistic audio cues, we developed a multi-stage curation pipeline to extract fine-grained, time-aligned signals from both modalities, resulting in 511K captioning samples (durations of 5–900s) and 266K parsing samples. This pipeline consists of three steps: (1) *Filtering.* We apply Voice Activity Detection (VAD) to remove silence, and Language Identification (LID) via SenseVoice An et al. (2024) to retain only English and Mandarin content. Clips with severe motion blur or durations shorter than 5 seconds are discarded. (2) *Temporal-Visual Segmentation.* To capture local dynamics, we perform Scene Boundary Detection based on chromatic and luminance variance between adjacent frames. The video is partitioned into semantic segments; clips under 3s or 5 frames are pruned, while those over 60s are sub-segmented. For each segment, we extract visual attributes (atomic actions, object-actor interactions, and basic camera motion) and use Qwen3-VL-235B-A22B to generate detailed event descriptions. (3) *Cross-Modal Synthesis and Structured Representation.* We fuse unimodal streams into a structured hierarchy by calculating the intersection of visual boundaries and audio semantic chunks. At the *segment-level*, the data contains timestamped descriptions paired with visual attributes and audio semantic tags (e.g., "Instrumental Music", "Human Voice"). At the *global-level*, combining Qwen3-VL-235B-A22B with MidasHengLM, we employ dynamic, category-aware schemas to synthesize a holistic video narrative that integrates the full speaker-attributed ASR history. This structured output reduces redundancy and enforces

---

cross-modal consistency, transforming audio from a secondary text source into a primary sensory channel for identity, environment, and narrative context.

- **Camera-aware Video.** While the general data captures overarching visual attributes, deep cinematic understanding requires precise spatiotemporal grounding of camera dynamics (e.g., distinguishing fast tracking shots from slow dolly-in shots). To equip MLLMs with this capability, we construct a 191K-sample dataset (4–10 s duration) sourced from MovieNet Huang et al. (2020) and internal datasets. To mitigate the unreliability of automated estimators, we adopt a hybrid pipeline: VGGT Wang et al. (2025b) provides automated coarse filtering, followed by professional manual annotation of  $\sim 50\text{K}$  clips. The annotation utilizes a two-level taxonomy adapted from CameraBench Lin et al. (2025): L1 categorizes broad motions into *no-motion*, *tracking*, and *non-tracking*; L2 refines *tracking* into 7 subclasses (e.g., pan/tilt/arc tracking) and *non-tracking* into 15 subclasses covering specific translations, rotations, and focal adjustments. Based on these high-precision labels, Qwen3-Omni-30B-A3B synthesizes camera-aware descriptions and temporal parsing boundaries, while Gemini-2.5-Pro generates reasoning-oriented QA pairs. This dedicated corpus significantly enhances the models’ temporal precision and capability to integrate complex camera movements into narrative descriptions.

**Text-Rich Videos.** To address the critical need for fine-grained semantic parsing and structured understanding in long-form, text-rich instructional videos, we construct an in-house course video dataset. Specifically, this includes 130K in-depth structured captions, and 79K course video parsing entries. Videos are collected from high-quality educational channels on YouTube, covering university open courses, foundational discipline series, professional skills training, and popular science lectures across multiple domains such as technology, business, humanities, and arts. We use Qwen3-Omni-30B-A3B for data curation, retaining videos with clear objectives, high knowledge density, and rich audio-visual signals.

- **In-Depth Structured Caption.** We generate course reports with a two-step pipeline: (1) Qwen3-Omni-30B-A3B summarizes audio content; (2) Qwen3-VL-235B-A22B fuses the audio summaries with visual content to produce a structured report following a predefined template. The template includes five core dimensions: course title, core abstract, structured outline (via logical sectioning), deep content mining (core concepts, Q&A, and resources such as code, formulas, and charts), and learning path planning. It significantly enhanced the model’s capacity for information distillation and structured summarization in long-form dynamic audio-visual scenarios.
- **Parsing.** We build an automated parsing pipeline to convert fragmented data into structured information: (1) keyframe and timestamp extraction using SSIM Zhang et al. (2025); (2) fine-grained OCR on keyframes with Qwen3-VL-235B-A22B to accurately extract LaTeX formulas, Markdown tables, format-preserved code blocks, titles, and standard text paragraphs, yielding a series of chronologically ordered frame-level OCR results; (3) semantic-aware temporal aggregation via Qwen3-235B-A22B-Thinking to transform discrete keyframes into continuous semantic segments by dynamically detecting contextual boundaries and intelligently merging evolving content (e.g., stitching scrolling code, updating dynamic tables, and eliminating redundancies); (4) segment-level audio processing using Qwen3-Omni-30B-A3B to extract corresponding audio annotations (including both ASR transcripts and audio captions), integrating these modalities into the localized parsing results; and (5) global audio-visual caption, wherein Qwen3-Omni-30B-A3B first generates a holistic audio description from the full audio track, which is subsequently inputted alongside the video into Qwen3-VL-235B-A22B to yield a comprehensive global description. Ultimately, this pipeline generates a unified JSON dataset formatted as follows: a chronologically ordered series of segments—each comprising a start and end timestamp, consolidated OCR text, and localized audio annotations (available in two modes: ASR or audio caption)—terminating with the overarching global audio-visual description appended at the end. This pipeline effectively transforms long-sequence, complex audio-visual streams into precisely structured, temporally aligned multimodal knowledge.

### 2.3 TRAINING

To train Logics-Parsing-Omni as a unified parser that seamlessly integrates localized structural fidelity with high-level semantic interpretation, we initialize our model from Qwen3-Omni-30B-A3B, which has established a robust baseline across a wide range of cross-modal tasks. Instead of training from scratch, we adopt a two-stage progressive training strategy that perfectly mirrors our Omni

---

Parsing framework. Standard autoregressive next-token prediction is used as the supervised fine-tuning (SFT) objective in both stages.

**Stage 1: Large-scale Multitask Capability & Knowledge Expansion.** The core objective of this stage is to construct a “Panoramic Cognitive Foundation.” Leveraging a curated large-scale dataset of 16M supervised samples, we perform full-parameter SFT. In this phase, we do not enforce strict category balancing; instead, we prioritize data scale and coverage to build the foundational skills for Holistic Detection (L1) and Fine-grained Recognition (L2):

- *Visual Knowledge Injection:* We introduce approximately 12.6 million image-based QA pairs to map visual features into an encyclopedic world knowledge space. This encourages the model to not only “perceive” entities but also intuitively associate them with underlying high-level semantic facts, thereby expanding its cognitive breadth.
- *Atomic Capability Generalization:* We aggregate data from diverse foundational tasks, including document structure parsing, knowledge-aware natural image captioning, image/geometric editing difference captioning, chart/graphics captioning, as well as general audio and audio-visual captioning. This comprehensive exposure ensures the model masters pure structural parsing and basic semantic descriptions before being overwhelmed by complex reasoning tasks.

Following Stage 1, the model accumulates extensive knowledge reserves and preliminary cross-task generalization capabilities. However, due to the sheer volume of image QA data, the model exhibits certain task distribution biases and has yet to fully master the highly structured logical reasoning required by our paradigm. To unlock its precision potential, we proceed to the second stage.

**Stage 2: Unified Parsing Alignment & Balanced Instruction Tuning.** To rectify the task distribution bias inherited from Stage 1 and achieve deep integration of perception and cognition (i.e., L3 Semantic Interpretation), we shift our training paradigm from scale-driven knowledge accumulation to precise, balanced instruction tuning. By constructing a high-quality dataset comprising 5M samples, we explicitly prioritize instruction density, data quality, and structural diversity:

- *Multi-domain Task Reinforcement:* The cornerstone of this stage is the high-quality data synthesized by our Omni Parsing Framework (as illustrated in Figure 4). This activates the full L1-to-L3 progressive parsing pipeline across all domains detailed in our corpus. Specifically, it includes: document parsing (covering pure structural and joint structure-semantic extraction); image parsing (encompassing natural images, knowledge-aware images, and graphics, with tasks spanning single-image and multi-image difference parsing); general audio parsing; and comprehensive video parsing (spanning natural, camera-aware, and text-rich videos). To preserve the model’s general conversational capabilities, we also integrate a minor, meticulously balanced proportion of multi-modal captioning and QA data.
- *Omni-modal Schema Alignment:* Through fine-tuning on this strictly balanced distribution, we achieve a dual alignment of structured extraction and free-form semantic interaction. For omni-parsing tasks, we explicitly enforce a unified output schema, training the model to map heterogeneous inputs—whether documents, static images, or dynamic audio-visual streams—into standardized JSON formats that seamlessly bridge spatial-temporal grounding with semantic reasoning. Concurrently, it maintains fluent natural language generation for general QA and captioning. Consequently, the model learns to process omni-modal signals under a rigorous progressive parsing paradigm without sacrificing its conversational versatility.

Ultimately, this two-stage methodology ensures that Logics-Parsing-Omni not only inherits vast encyclopedic knowledge but also demonstrates highly consistent instruction-following capabilities. It successfully realizes the efficient synergy between fine-grained pixel/signal-level perception and high-level semantic cognition, achieving the optimal state designed by our framework.

**Experimental settings.** We implemented our framework using Megatron-SWIFT Zhao et al. (2024) across both training stages. For model architecture, we unfroze all components of Qwen3-Omni-30B-A3B except the talker, including all parameters of the LLM, vision encoder, audio encoder, and aligners. For multimodal data processing, we established precise input specifications for distinct modalities: images retain their original aspect ratio and resolution; for videos, we applied a uniform sampling rate of 2.0 FPS, set the maximum number of extracted frames to 768, and utilized the original resolution for individual frames. To further enhance computational efficiency and ensure load balancing during multimodal long-sequence training, we introduced a sequence packing strategy, maintaining a constant global batch size of 32 and extending the maximum sequence length to 56k

to fully accommodate the contextual requirements of long documents and audio-visual inputs. The optimization process employed a base learning rate of  $1e-5$ , coupled with a warmup ratio of 0.05 and a cosine decay strategy, to achieve smooth convergence during model training.

### 3 EVALUATION

#### 3.1 OMNIPARSINGBENCH

##### 3.1.1 OVERALL

To rigorously evaluate the unified parsing capabilities of our model across diverse modalities, we construct OmniParsingBench, a comprehensive, large-scale, and high-quality evaluation corpus. Unlike traditional single-task benchmarks, OmniParsingBench is designed to assess the full spectrum of parsing performance—from fundamental signal detection to complex semantic reasoning—across six primary domains: Document, Natural Image, Graphics, Audio, Natural Video and Text-Rich Video.

Our evaluation framework strictly aligns with the proposed three-stage architecture (L1–L3), systematically assessing performance from L1-Holistic Detection (spatio-temporal grounding and classification), L2-Fine-grained Recognition (symbol extraction, attribute identification, and structural recovery), to L3-Multi-level Interpreting (semantic consistency and hallucination resistance). To provide a concise view of model capabilities, we aggregate these fine-grained metrics into two core scores: Perception, which evaluates signal precision and structural fidelity (dominating L1 and L2), and Cognition, which evaluates logical reasoning and semantic understanding (dominating L3).

As detailed in Table 2, Logics-Parsing-Omni demonstrates highly competitive or state-of-the-art capabilities across all six diverse modalities when evaluated on Overall (Ovr.), Perception (Perc.), and Cognition (Cog.) metrics. Notably, our model consistently surpasses all evaluated baselines—including the leading proprietary Gemini-3-Pro—in the Overall and Cognition metrics of the Graphics and Audio domains, as well as across all metrics in Text-Rich Video. This superiority is particularly pronounced in the Cognition metric, where Logics-Parsing-Omni exhibits exceptional logical reasoning and semantic understanding, achieving top-tier scores such as 92.19 in Graphics and 79.03 in Text-Rich Video. While Gemini-3-Pro maintains an advantage in the fundamental perception of Natural Images, Graphics, Audio, and Documents, as well as a marginal lead in Natural Video, our model significantly outperforms other open-weight counterparts (e.g., the Qwen series) in nearly all metrics. These quantitative results validate the efficacy of our L1–L3 architecture, demonstrating that Logics-Parsing-Omni successfully bridges fundamental signal detection with complex multi-modal interpreting.

Table 2: Performance comparison of various models on OmniParsingBench.

Model	Natural Image			Graphics			Document	Audio			Natural Video			Text-Rich Video		
	Ovr.	Perc.	Cog.	Ovr.	Perc.	Cog.	Perc.	Ovr.	Perc.	Cog.	Ovr.	Perc.	Cog.	Ovr.	Perc.	Cog.
Gemini-3-Pro	<b>69.72</b>	<b>63.15</b>	<b>76.29</b>	<u>86.66</u>	<b>85.33</b>	87.98	<b>87.01</b>	<u>52.68</u>	<b>73.99</b>	31.37	<b>44.56</b>	<b>52.54</b>	<b>36.57</b>	<u>61.00</u>	<u>53.47</u>	<u>68.53</u>
GPT-5.2	52.84	46.07	59.61	81.07	70.34	<u>91.80</u>	77.43	-	-	-	-	-	-	-	-	-
Qwen3.5-397B-A17B	54.80	47.12	62.48	78.79	74.44	83.15	81.09	-	-	-	-	-	-	-	-	-
Qwen3-VL-235B-A22B	59.34	<u>50.62</u>	68.05	78.00	72.15	83.85	84.47	-	-	-	-	-	-	-	-	-
Qwen3-VL-30B-A3B	53.73	46.47	60.99	73.05	66.31	79.78	78.94	-	-	-	-	-	-	-	-	-
Qwen3-Omni-30B-A3B	51.30	44.88	57.72	74.93	71.39	78.47	73.50	48.17	62.86	<u>33.48</u>	27.98	29.35	26.60	25.06	8.40	41.72
Logics-Parsing-Omni(Ours)	<u>62.46</u>	50.53	<u>74.38</u>	<b>87.43</b>	<u>82.67</u>	<b>92.19</b>	<u>84.90</u>	<b>53.75</b>	<u>70.03</u>	<b>37.48</b>	<u>43.78</u>	<u>51.76</u>	<u>35.79</u>	<b>66.78</b>	<b>54.52</b>	<b>79.03</b>

Note: Bold text indicates the best result, and underlined text indicates the second-best result.

##### 3.1.2 IMAGE

**Natural Images.** To rigorously assess the perceptual and cognitive capabilities of models on natural images, we utilize the Natural Image module of OmniParsingBench. This subset comprises 1,000 diverse natural images alongside 1,000 images annotated with authoritative domain knowledge (covering domains that require knowledge-aware parsing, such as landmark buildings, brands, and biological species). To ensure structural compatibility across heterogeneous model architectures, all models must output their parsing results in a predefined structured format. Comprehensive

details regarding dataset curation, evaluation protocols, metric formulations, and extended results are provided in Appendix A.1.

The evaluation metrics are systematically structured along two core dimensions:

- **Perception:** This aspect assesses the model’s fundamental signal detection and symbol extraction capabilities across two sequential stages: (1) *Location*: Quantifies spatial grounding ability by calculating the mean localization recall (IoU >0.5) for general entities, knowledge-aware entities, and text blocks. (2) *Content*: Applies rigorous exact-match and semantic verification to successfully localized instances. This includes evaluating the semantic fidelity of general entities, ensuring exact OCR and language-type matching for text, and verifying that knowledge-aware entities accurately reference their authoritative identifiers.
- **Cognition:** This aspect evaluates the logical coherence, depth, and hallucination resistance of the global captions derived from the parsed structures. It is subdivided into: (1) *General Caption QA*: Following the CaptionQA protocol, an LLM evaluates the global description across nine multidimensional semantic aspects (e.g., theme, spatial relationships, textual content, visual style) using grounded question-answer pairs. (2) *Knowledge Reference*: For images containing knowledge-aware entities, this metric computes the proportion of captions that explicitly and accurately integrate all verified knowledge identifiers into the global narrative, thereby ensuring factual correctness and structural-semantic alignment.

Table 3: Evaluation results on the Natural Image module of OmniParsingBench.

Model	Overall <sup>‡</sup>	Perception					Cognition		
		Location	Content*			Avg.	General	Knowledge	Avg.
			Entity	Knowledge	Text				
Gemini-3-Pro <sup>13</sup>	<b>69.72</b>	<b>78.33</b>	<b>98.64</b>	<u>75.69</u>	<b>67.15</b>	<b>63.15</b>	<u>89.87</u>	<b>62.70</b>	<b>76.29</b>
GPT-5.2 <sup>19</sup>	52.84	66.15	95.19	–	47.20	46.07	81.72	37.50	59.61
Qwen3.5-397B-A17B <sup>16</sup>	54.80	63.71	97.42	<b>80.41</b>	52.25	47.12	76.46	48.50	62.48
Qwen3-VL-235B-A22B Bai et al. (2025a)	59.34	68.66	97.85	68.61	60.63	<u>50.62</u>	82.70	53.40	68.05
Qwen3-VL-30B-A3B Bai et al. (2025a)	53.73	67.52	97.51	57.37	59.61	46.47	75.68	46.30	60.99
Qwen3-Omni-30B-A3B Xu et al. (2025b)	51.30	63.10	<u>97.92</u>	58.27	60.08	44.88	74.34	41.10	57.72
Logics-Parsing-Omni (Ours)	<u>62.46</u>	<u>69.58</u>	97.88	59.81	<u>62.49</u>	50.53	<b>90.36</b>	<u>58.40</u>	<u>74.38</u>

\* Content metrics are semantic accuracy computed conditionally on successfully localized instances.

<sup>‡</sup> Overall Score = mean(Perception Avg, Cognition Avg.).

<sup>†</sup> GPT-5.2 exhibits policy-induced constraints in knowledge identification; Knowledge Score is excluded in Avg. Score.

**Result Analysis.** As shown in Table 3, **Logics-Parsing-Omni** achieves an Overall score of 62.46%, outperforming all evaluated open-weight models (e.g., Qwen3-VL-235B-A22B at 59.34%) and demonstrating a highly competitive balance between structural fidelity and semantic understanding.

For the Perception (Avg. 50.53%), our model excels in signal detection with a leading Location score of 69.58% among open-weight models, while maintaining robust general entity and text recognition. For the Cognition (Avg. 74.38%), Logics-Parsing-Omni exhibits exceptional semantic depth. Notably, it achieves a state-of-the-art General Caption score of 90.36%, surpassing even the proprietary Gemini-3-Pro (89.87%). This confirms our framework produces logically coherent and factual narratives (Knowledge Ref. 58.40%) driven by explicit structured parsing rather than hallucination.

**Graphics.** To rigorously evaluate the perceptual and cognitive capabilities of models on information-dense visual elements, we conduct our evaluation on the Graphics module of Omni-ParsingBench. This subset encompasses two highly structured domains requiring complex spatial and logical deduction: Charts and Geometric Figures. Consistent with our overall evaluation framework, we specifically instantiate the Perception and Cognition dimensions for the Graphics module as follows:

- **Perception:** This dimension evaluates fundamental visual decomposition and exact structural recovery. It is subdivided into: (1) *Location*: Assesses precise geometric spatial positioning (e.g., exact coordinates and radii). (2) *Content - Element*: Evaluates the extraction of fundamental geometric primitives (points, lines, circles). (3) *Content - Relation*: Measures the extraction of explicit topological and quantitative relationships in geometry. (4) *Content - Chart*: Evaluates struc-

tural reverse-rendering exactness, measuring data extraction in statistical charts (via F1-score) and topological correctness in structural diagrams (via Mermaid similarity).

- **Cognition:** This dimension assesses the model’s ability to bind visual structures with mathematical or factual logic. Following the CaptionQA protocol used in Natural Images, an LLM evaluates semantic coverage and reasoning capabilities using grounded question-answer pairs. It is subdivided into: (1) *Element*: Evaluates fundamental information extraction across both domains (e.g., basic geometric elements and chart OCR data). (2) *Relation*: Captures the ability to comprehend and bind complex topological and visual structures. (3) *Reasoning*: Represents complex logical deduction capability, specifically the ability to analyze implicit data trends, fluctuations, and perform numerical reasoning in charts.

Table 4: Evaluation results on the Graphics Module of OmniParsingBench.

Model	Overall	Perception					Cognition			
		Location	Content			Avg.	Element	Relation	Reasoning	Avg.
			Element	Relation	Chart					
Gemini-3-Pro	86.66	80.04	<b>87.38</b>	<b>86.12</b>	87.80	<b>85.33</b>	90.48	90.35	83.11	87.98
GPT-5.2	81.07	45.84	<u>84.31</u>	67.66	83.56	70.34	<u>92.38</u>	89.08	<b>93.95</b>	<u>91.80</u>
Qwen3.5-397B-A17B	78.79	46.70	83.01	<u>76.13</u>	<b>91.91</b>	74.44	86.48	88.99	73.97	83.15
Qwen3-VL-235B-A22B	78.00	52.82	84.17	67.62	83.99	72.15	86.69	83.12	81.74	83.85
Qwen3-VL-30B-A3B	73.05	62.34	82.10	53.41	67.40	66.31	82.67	82.26	74.43	79.78
Qwen3-Omni-30B-A3B	74.93	60.17	82.76	56.44	86.19	71.39	81.22	80.22	73.97	78.47
Logics-Parsing-Omni (Ours)	<b>87.43</b>	<b>86.30</b>	83.34	72.91	<u>88.12</u>	<u>82.67</u>	<b>96.16</b>	<b>92.27</b>	<u>88.13</u>	<b>92.19</b>

*Result Analysis.* As shown in Table 4, Logics-Parsing-Omni achieves an overall accuracy of 87.43, showing a significant improvement over the baseline Qwen3-Omni-30B-A3B (74.93) and demonstrating strong competitiveness against state-of-the-art models. For the Perception, our model attains an exceptional score of 86.30 in fine-grained Location, significantly outperforming Gemini-3-Pro and GPT-5.2.

Anchored by this precise structural perception, Logics-Parsing-Omni dominates the Cognition, achieving the highest average accuracy of 92.19. Notably, our model excels in fundamental extraction and structural binding, achieving state-of-the-art scores in both the Element (96.16) and Relation (92.27) metrics. Furthermore, in the complex Reasoning metric—which evaluates logical deduction capabilities—our model reaches a highly competitive 88.13, surpassing Gemini-3-Pro (83.11) and closely following GPT-5.2 (93.95).

These results validate our proposed progressive parsing paradigm: the fine-grained structural fidelity helps mitigate the limitations of superficial image captioning, laying a robust foundation for rigorous spatial deduction and complex logical reasoning. Detailed evaluation dimensions and results are provided in Appendix A.2.

### 3.1.3 DOCUMENT

In this subsection, we report the experimental results of our Logics-Parsing-Omni model on the proposed LogicsDocBench<sup>14</sup>, which effectively validates the effectiveness of the proposed omni model on the document parsing task. To be specific, LogicsDocBench contains 900 carefully curated page-level PDF images covering both traditional Parsing-1.0 tasks and newly introduced Parsing-2.0 scenarios, including flowcharts, music sheets and pseudo-code blocks. Since our omni model does not include Parsing-2.0 scenarios training, we only report the evaluation results on Parsing-1.0 tasks. Quantitative comparison results are summarized in Table 5.

*Result Analysis.* From the experimental results presented in Table 5, we observe that our proposed Logics-Parsing-Omni model outperforms all Qwen-series models by a large margin, including Qwen3-Omni-30B-A3B, Qwen3-VL-30B-A3B and the newly released Qwen3.5-397B-A17B, which highlights its superior capability in complex document parsing. Although slightly inferior to Gemini-3-Pro, Logics-Parsing-Omni surpasses all other general-purpose vision-language large models (VLMs), as well as some of the specialized OCR-focused models, such as dots.ocr, DeepSeek-OCR series and so on. These experimental results provide strong evidence of the effectiveness and robustness of Logics-Parsing-Omni as a generalized VLM in handling challenging, real-world doc-

Table 5: Comprehensive evaluation of document reading on LogicsDocBench.

Model	Perception					
	Overall $\uparrow$	Text <sup>Edit</sup> $\downarrow$	Formula <sup>CDM</sup> $\uparrow$	Table <sup>TEDs</sup> $\uparrow$	Table <sup>TEDSs</sup> $\uparrow$	Reading Order <sup>Edit</sup> $\uparrow$
<b>Pipeline</b>						
MinerU2-pipeline Wang et al. (2024a)	77.93	0.1013	75.89	68.03	76.14	0.2157
MinerU2.5 Niu et al. (2025)	<u>86.30</u>	0.0754	<b>85.07</b>	81.36	84.48	0.1334
PP-StructureV3 Cui et al. (2025b)	70.26	0.1155	78.20	44.12	74.65	0.1891
PaddleOCR-VL Cui et al. (2025a)	85.09	<b>0.0581</b>	83.80	77.27	81.60	0.1404
PaddleOCR-VL-1.5 Cui et al. (2026)	85.43	<u>0.0587</u>	82.78	79.38	84.30	<u>0.1212</u>
MonkeyOCR-pro-1.2B Li et al. (2025)	77.57	0.1653	79.85	69.39	74.77	0.2788
GLM-OCR <sup>15</sup>	85.59	0.0689	84.10	79.57	83.90	0.1490
<b>End-to-end Model</b>						
Qwen3-Omni-30B-A3B Xu et al. (2025b)	73.50	0.2093	72.07	69.37	73.49	0.2317
HunyuanOCR Team et al. (2025a)	76.11	0.1504	71.62	71.75	76.47	0.2036
DeepSeek-OCR Wei et al. (2025)	74.45	0.1650	76.90	62.94	66.76	0.2189
DeepSeek-OCR 2 Wei et al. (2026)	77.04	0.1111	76.92	65.32	70.48	0.1554
InternVL35-241B Wang et al. (2025c)	76.03	0.2035	83.23	65.21	72.00	0.2138
GPT-5.2 <sup>9</sup>	77.43	0.2072	83.41	69.61	74.60	0.2148
Qwen3-VL-30B-A3B Bai et al. (2025a)	78.94	0.1340	81.52	68.69	75.33	0.1718
Qwen3.5-397B-A17B <sup>16</sup>	81.09	0.0868	80.37	71.57	78.48	0.1450
Gemini-2.5-Pro Comanici et al. (2025)	84.29	0.0985	81.07	<u>81.64</u>	<u>87.67</u>	0.1689
dots.ocr <sup>6</sup>	84.51	0.0629	81.60	78.21	82.49	<b>0.1153</b>
Qwen3-VL-235B-A22B Bai et al. (2025a)	84.47	0.0817	84.00	77.58	81.92	0.1405
Gemini-3-Pro <sup>13</sup>	<b>87.01</b>	0.0815	<u>84.86</u>	<b>84.33</b>	<b>90.66</b>	0.1468
Logics-Parsing-Omni (Ours)	84.9	0.0666	80.41	80.93	84.25	0.1223

ument parsing tasks. Furthermore, specific visual examples of the evaluated cases are provided in the Appendix (see Fig. 16 and Fig. 17).

### 3.1.4 AUDIO

To rigorously evaluate the capabilities of models in fine-grained parsing and comprehensive understanding within audio-only scenarios, we introduce the Audio Module of OmniParsingBench. The benchmark comprises 2 main tasks (perception and cognition) and 5 detailed task types, encompassing a total of 2434 cases.

- **Perception.** To evaluate the model’s ability to identify audio categories and their precise temporal boundaries.
  - **Data Construction.** (1) *Audio Event Detection* cases were stochastically sampled from the AudioSet-strong Hershey et al. (2021) dataset. For evaluation clarity, we re-categorized the labels into six primary classes: Human Voice, Instrumental Music, Environmental Noise, Traffic, Animals, and Daily Life Sounds. This task is further bifurcated into *Identity Recognition*

<sup>1</sup><https://doc2x.noedgeai.com/>

<sup>2</sup><https://www.textin.com>

<sup>3</sup><https://mathpix.com/>

<sup>4</sup><https://github.com/datalab-to/marker>

<sup>5</sup><https://github.com/breezedeus/Pix2Text>

<sup>6</sup><https://github.com/rednote-hilab/dots.ocr>

<sup>7</sup><https://ocrflux.pdfparser.io/>

<sup>8</sup>[https://seed.bytedance.com/zh/seed1\\_6](https://seed.bytedance.com/zh/seed1_6)

<sup>9</sup><https://openai.com/zh-Hans-CN/index/introducing-gpt-5/>

<sup>10</sup><https://mistral.ai/news/mistral-ocr>

<sup>11</sup>[https://github.com/lavvsharma/ocr\\_verse](https://github.com/lavvsharma/ocr_verse)

<sup>12</sup><https://openai.com/zh-Hans-CN/index/hello-gpt-4o/>

<sup>13</sup><https://aistudio.google.com/models/gemini-3>

<sup>14</sup><https://github.com/alibaba/Logics-Parsing>

<sup>15</sup><https://github.com/zai-org/GLM-OCR>

<sup>16</sup><https://github.com/QwenLM/Qwen3.5>

and *Temporal Localization*. (2) ASR samples were randomly selected from the Librispeech Panayotov et al. (2015) corpus to serve as the ground truth for speech transcription.

- **Evaluation Metrics.** The perception task utilizes Key F1 and Time F1 metrics, calculated using a Macro Average across two dimensions. (1) *Key-level Metrics*: To assess category-level performance, we calculate Key F1 by balancing Key Recall (the fraction of ground truth keys detected) and Key Precision (the fraction of predicted keys that are correct). (2) *Time-level Metrics*: Time-based F1 score is derived from Time Recall and Time Precision, which measure the temporal overlap between predicted segments and ground truth intervals relative to their total durations. (3) *ASR WER*: It is employed to measure the linguistic accuracy of the model’s transcriptions against the ground truth.
- **Cognition.** To assess the model’s high-level semantic understanding and reasoning capabilities regarding audio content.
  - **Data Construction.** The cognition set is a hybrid corpus consisting of the Worldsense Hong et al. (2025) dataset and a self-constructed dataset. The latter was generated following the pipeline described in 2.2.3, where Gemini-3-flash-preview processed segmented audio to generate complex Question-Answering (QA) pairs.
  - **Subtasks.** The cognition task focuses on two core dimensions. (1) *Audio Information Extraction*: The ability to distill specific information and key details from complex audio environments. (2) *Audio Recognition*: Evaluating the model’s deeper comprehension and logical interpretation of audio events.

Table 6: Evaluation results on the Audio Module of OmniParsingBench

Model	Overall	Perception				Cognition		
		Time	Key	ASR↓	Avg.	Info. Ext.	Rec.	Avg.
Gemini-3-Pro	<u>52.68</u>	<b>51.49</b>	<b>72.49</b>	<b>0.0201</b>	<b>73.99</b>	<u>9.17</u>	53.57	31.37
Qwen3-Omni-30B-A3B	48.17	41.25	51.69	0.0437	62.86	8.62	<u>58.33</u>	<u>33.48</u>
Logics-Parsing-Omni(Ours)	<b>53.75</b>	<u>50.04</u>	<u>62.34</u>	<u>0.0230</u>	<u>70.03</u>	<b>9.48</b>	<b>65.48</b>	<b>37.48</b>

Note: Bold text indicates the best result, and underlined text indicates the second-best result.

*Result Analysis.* As summarized in Table 6, the overall score is aggregated from Perception and Cognition dimensions. The exact calculation rules are detailed in Appendix A.3. Logics-Parsing-Omni establishes a new state-of-the-art (SOTA) on the Audio Module of OmniParsingBench with an overall score of 53.75. In the cognition tasks, it achieves 9.48% accuracy in audio information extraction and 65.48% in audio recognition—surpassing the strongest baseline by a significant 11.91% margin—which underscores its exceptional semantic comprehension. Qualitatively (Figure 5), the model demonstrates robust parsing capabilities by generating structured JSON outputs with high-precision timestamps and tags, complemented by descriptive captions that effectively capture the dynamic progression of the auditory scene.

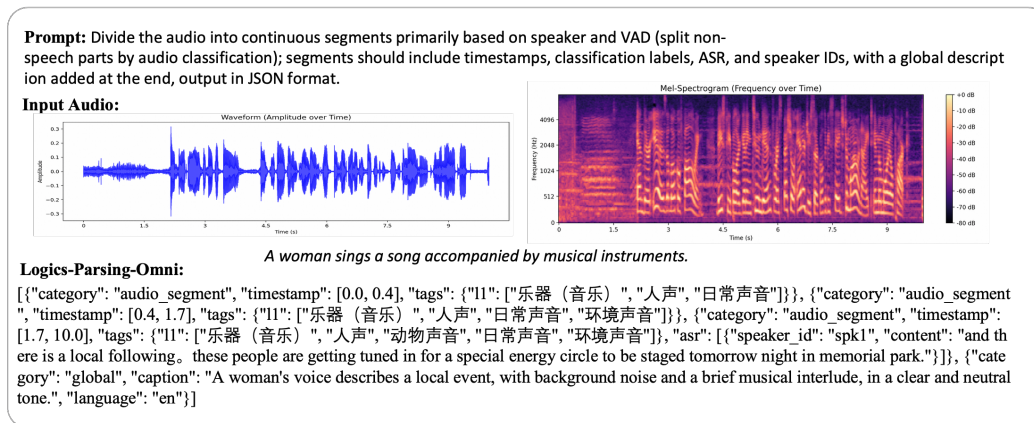


Figure 5: Qualitative examples illustrating the comprehensive audio parsing capability of Logics-Parsing-Omni.

### 3.1.5 VIDEO

**Natural Videos.** We construct the Natural Video module of OmniParsingBench, which includes over 1,100 samples covering perception and cognition (sourced from the Worldsense dataset and newly curated YouTube multi-turn QA) as well as 725 strictly controlled single-motion scenes (330 L1 and 395 L2). The comprehensive evaluation results are summarized in Table 7. The exact calculation rules are detailed in Appendix A.4. We evaluate these scenarios across two core dimensions:

- **Perception:** This dimension evaluates the model’s accuracy in capturing low-level audio-visual details and recognizing technical terminology. The evaluation covers three core aspects:
  - *Audio-centric parsing:* Assesses identity recognition and speech-to-text accuracy (ASR WER).
  - *Temporal Grounding:* Evaluates the precision of audio-visual temporal localization and ordered video event detection, which requires the model to accurately identify events while maintaining their correct chronological sequence.
  - *Camera Motion Analysis:* Measures the classification accuracy of professional camera terminology (L1/L2 motions) and their joint prediction performance.
- **Cognition:** This dimension moves beyond basic parsing to assess complex reasoning capabilities and the natural integration of multi-modal concepts into language. The evaluation is categorized into three cross-modal reasoning aspects:
  - *Audio Reasoning:* Evaluates auditory semantic understanding, including acoustic event counting, semantic sound recognition, and complex audio information extraction.
  - *Visual Semantics & Dynamics:* Assesses visual-centric comprehension, such as attribute recognition and event description. Crucially, it also evaluates the natural integration of spatial-dynamic concepts (i.e., camera motion) into global video captions. To ensure robust evaluation of these dynamic descriptions, we adopt an LLM-as-a-Judge paradigm (Qwen3-235B-A3B) to validate semantic consistency by mapping descriptions into eight macro motion concepts (e.g., zoom in/out, pan, track), rather than relying on strict lexical matching.
  - *Audio-Visual Reasoning:* Tests the model’s ability to synthesize information across modalities, focusing on complex tasks like audio-visual emotion change analysis and causal reasoning (i.e., understanding the underlying physical relationship between specific sounds and visual actions).

Table 7: Evaluation results on the Natural Video Module of OmniParsingBench, integrating both General Videos and Camera-aware Videos metrics.

Model	Overall	Perception						Cognition								
		Time	Key	ASR↓	Visual	Camera	Avg.	Audio			Visual		Audio-Visual		Avg.	
								Count	Rec.	Info. Ext.	Attr.& States	Event	Camera	Emot.		Caus. Rsn.
Gemini-3-Pro	<b>44.56</b>	<b>69.30</b>	<b>78.13</b>	<b>0.2148</b>	2.96	<u>33.79</u>	<b>52.54</b>	<u>14.29</u>	<b>39.25</b>	<b>36.61</b>	<b>31.76</b>	<b>29.00</b>	<u>47.31</u>	<u>55.56</u>	<b>38.79</b>	<b>36.57</b>
Qwen3-Omni-30B-A3B	27.98	35.89	52.94	0.6578	<b>5.93</b>	17.79	29.35	11.90	25.23	<u>26.79</u>	20.00	<u>26.00</u>	38.21	42.22	22.41	26.60
Logics-Parsing-Omni(Ours)	<u>43.78</u>	<u>55.47</u>	<u>61.35</u>	<u>0.2413</u>	<u>5.43</u>	<b>60.69</b>	<u>51.76</u>	<b>20.24</b>	<u>30.84</u>	<u>26.79</u>	<u>29.41</u>	25.00	<b>68.69</b>	<b>57.78</b>	<u>27.59</u>	<u>35.79</u>

*Note:* Bold text indicates the best result, and underlined text indicates the second-best result.

*Result Analysis.* As indicated by Table 7, Logics-Parsing-Omni demonstrates highly competitive capabilities across both perception and cognition dimensions, achieving an Overall score of 43.78. This closely rivals the leading closed-source model Gemini-3-Pro (44.56) and significantly surpasses the Qwen3-Omni-30B-A3B baseline (27.98).

In the **Perception** dimension, the model exhibits overwhelming superiority in *Camera Motion Analysis*, attaining a joint terminology accuracy of 60.69%, which outperforms Gemini-3-Pro (+26.9%) and Qwen3-Omni-30B-A3B (+42.9%) by massive margins. For fine-grained *Audio-centric parsing* (e.g., identity recognition, ASR) and *Temporal Grounding*, it consistently secures robust second-best results, demonstrating a solid foundation in low-level feature capture.

In the **Cognition** dimension, Logics-Parsing-Omni establishes state-of-the-art performance across diverse cross-modal reasoning tasks. Within *Audio Reasoning*, it achieves an optimal 20.24% in acoustic event counting. For *Visual Semantics & Dynamics*, the model proves its exceptional capacity for macro-level semantic alignment by achieving a top-tier camera captioning accuracy of 68.69% (+21.38% over the strongest baseline). Furthermore, in complex *Audio-Visual Reasoning*, it leads the benchmark with 57.78% in emotion change analysis.

Qualitatively (Figures 13 and Figure 6), the model generates structured JSON outputs that seamlessly synchronize auditory events and hierarchical camera tags with visual sequences via high-precision timestamps. Simultaneously, it produces rich multimodal narratives that effectively weave physical spatial dynamics and the complex interplay between sound and action into cohesive global descriptions. Comprehensive details regarding the extended results are provided in Appendix A.4.



Figure 6: Qualitative examples illustrating the comprehensive camera-aware video parsing capability of Logics-Parsing-Omni.

**Text-Rich Videos.** To comprehensively evaluate the fine-grained parsing and structured knowledge extraction capabilities of multimodal models in long-form, highly dynamic audio-visual scenarios, we introduce the Text-Rich Video Module of OmniParsingBench. Extending the pipeline from Section 2.2.4, this benchmark employs GPT-5.2 to generate high-fidelity ground truths via semantic temporal aggregation, and subsequently uses it as an automated evaluator for iterative data filtering. This process results in 452 high-quality evaluation pairs designed for parsing and structured captioning. To address both fine-grained parsing and deep understanding, we introduce a three-dimensional framework: the perception and cognition dimensions evaluate parsing performance, while the in-depth cognition dimension assesses structured captioning.

- **Perception:** Evaluates the model’s ability to accurately localize and recognize bottom-level multimodal signals, comprising three core metrics: (1) *Time-F1 Score*: Assesses the precision of temporal boundaries for OCR segments. We compute the temporal Intersection over Union (tIoU), and report the average F1 Score across 10 thresholds:  $\{0.5, 0.55, \dots, 0.95\}$ . (2) *Visual-OCR Score*: All segment-level OCR predictions are chronologically concatenated. The score is calculated as one minus the normalized text edit distance. (3) *Audio-ASR WER*: All segment-level ASR transcripts are concatenated to compute the Word Error Rate (WER).

- **Cognition:** Examines semantic understanding and reasoning over the global audio-visual stream. We adopt a CaptionQA format where Gemini-3-Pro generates 5 challenging QAs per video, conditioned on the ground truth global audio-visual description and the raw video. The model’s predicted global description is then fed alongside the question into Qwen3-235B-A3B to determine answer correctness and compute the accuracy metric. The QAs span 7 fine-grained abilities across three modalities: object recognition, OCR, attributes&states recognition, and events recognition for visual understanding; information extraction for audio understanding; along with information synthesis and causal reasoning for audio-visual understanding.
- **Cognition (In-Depth):** Evaluates the generation of long-form, high-density structured course reports. Paralleling the standard Cognition pipeline, it utilizes ground truth in-depth structured captions to prompt Gemini-3-Pro to generate 9 QA pairs per video. Qwen3-235B-A3B then answers these QAs based on the evaluated model’s predicted caption to compute an accuracy score. The QAs cover 3 categories with 9 fine-grained abilities: (1) core summary (teaching objectives, domain tags, key conclusions); (2) structured outline (structural logic, reasoning depth, and key element extraction); and (3) deep content mining (concept definitions and rigorous detail verification, requiring precise extraction of experimental variables, mathematical symbols, code parameters, or chart data).

Table 8: Evaluation results on the Text-Rich Video Module of OmniParsingBench

Model	Overall	Perception				Cognition								
		Time	Visual	Audio↓	Avg.	Audio		Visual			Audio-Visual		In-Depth Str. Cap.	Avg.
						Info. Ext.	Object	OCR	Attr.&States	Event	Info. Syn.	Caus. Rsn.		
Gemini-3-Pro	<b>61.00</b>	<u>22.8</u>	<u>52.6</u>	<b>0.15</b>	<u>53.47</u>	<u>57.92</u>	<u>26.14</u>	<u>39.04</u>	<u>14.45</u>	<u>41.80</u>	<b>66.30</b>	<b>79.95</b>	<b>90.54</b>	<u>68.53</u>
Qwen3-Omni-30B-A3B	25.06	3.50	21.69	1.21	8.40	8.04	3.98	6.68	1.56	7.79	9.51	11.08	76.50	41.72
Logics-Parsing-Omni(Ours)	<b>66.78</b>	<b>30.43</b>	<b>53.14</b>	<u>0.20</u>	<b>54.52</b>	<b>70.92</b>	<b>57.95</b>	<b>71.39</b>	<b>58.59</b>	<b>65.16</b>	<b>77.17</b>	<u>79.42</u>	<u>89.41</u>	<b>79.03</b>

Note: Bold text indicates the best result, and underlined text indicates the second-best result.

Table 9: Detailed evaluation results for the Cognition (In-Depth Str. Cap.) dimension on the Text-Rich Video Module of OmniParsingBench

Model	Overall	Category			Video Duration		
		Core Summary	Structured Outline	Deep Content Mining	Short (< 5 min.)	Medium (5–15 min.)	Long (15–30 min.)
Gemini-3-Pro	<b>90.54</b>	<b>97.57</b>	<b>90.98</b>	<b>88.33</b>	<u>92.82</u>	<b>92.55</b>	<b>86.57</b>
Qwen3-Omni-30B-A3B	76.50	93.58	76.77	71.96	88.72	79.00	63.85
Logics-Parsing-Omni(Ours)	<u>89.41</u>	<u>97.35</u>	<u>89.88</u>	<u>86.95</u>	<b>93.50</b>	<u>91.33</u>	<u>84.04</u>

Note: Bold text indicates the best result, and underlined text indicates the second-best result.

*Result Analysis.* As shown in Table 8, the overall score is aggregated from Perception and Cognition dimensions. The exact calculation rules are detailed in Appendix A.5. The results demonstrate that our proposed Logics-Parsing-Omni achieves the highest Overall score of 66.78%, substantially outperforming Qwen3-Omni-30B-A3B and surpassing the proprietary Gemini-3-Pro. Notably, Logics-Parsing-Omni dominates in both fine-grained multimodal perception (54.52%) and overall cognition (79.03%). This highlights our model’s distinct advantage in precise temporal localization and bottom-level signal recognition within highly dynamic audio-visual streams. Table 9 reports results on the Cognition (In-Depth Str. Cap.) dimension, where the Overall score is the absolute accuracy over all QAs. Gemini-3-Pro is slightly better on long videos, while Logics-Parsing-Omni is competitive overall and performs better on short videos. Overall, our model demonstrates robust dense knowledge extraction and long-form structured captioning, narrowing the gap between open-source models and commercial systems in educational scenarios.

To further illustrate these capabilities qualitatively, we present two showcase examples. Figure 14 visualizes a course parsing scenario, demonstrating the model’s ability to precisely localize temporal OCR segments and accurately recognize dense audio and visual-textual elements. Additionally, Figure 15 highlights its proficiency in in-depth cognition, where Logics-Parsing-Omni successfully generates highly structured, contextually rich long-form captions that encapsulate complex educational concepts.

### 3.2 PERFORMANCE ON PUBLIC BENCHMARKS

#### 3.2.1 OMNIDOCBENCH v1.5

Apart from the previously proposed LogicsDocBench, we also conduct experiments on the commonly used open-sourced OmniDocBench-v1.5 Niu et al. (2025) benchmark for more fair and intuitive comparisons. Compared to its previous version (v1.0), OmniDocBench-v1.5 incorporates 374 additional document pages, resulting in an expanded test set of 1,355 pages with a more balanced distribution between Chinese and English content. Furthermore, the benchmark introduces updated evaluation protocols, where Character Detection Matching (CDM) Wang et al. (2025a) methods are employed for math formulas recognition evaluation, as well as the overall scores are calculated by weighted combination of the text edit distance, formula CDM score and the table Tree Edit Distance Similarity (TEDS) score.

Table 10: Comparisons with State-of-the-art methods on OmniDocBench-v1.5.

Model Type	Methods	Overall $\uparrow$	Text Edit $\downarrow$	Formula CDM $\uparrow$	Table TEDS $\uparrow$	Table TEDS-S $\uparrow$	ReadOrder $\downarrow$
Pipeline Tools	Marker-1.8.2 <sup>4</sup>	71.3	0.206	76.66	57.88	71.17	0.250
	MinerU2-Pipe Wang et al. (2024a)	75.51	0.209	76.55	70.90	79.11	0.225
	PP-StructureV3 Cui et al. (2025b)	86.73	0.073	85.79	81.68	89.48	0.073
General MLLMs	GPT-4o <sup>10</sup>	75.02	0.217	79.70	67.07	76.09	0.148
	InternVL3 Zhu et al. (2025)	80.33	0.131	83.42	70.64	77.74	0.113
	InternVL3.5 Wang et al. (2025c)	82.67	0.142	87.23	75.00	81.28	0.125
	GPT-5.2 <sup>9</sup>	86.23	0.115	88.6	81.60	86.42	0.099
	Qwen2.5-VL-72B Bai et al. (2025b)	87.02	0.094	88.27	82.15	86.22	0.102
	Gemini-2.5-Pro Comanic et al. (2025)	88.03	0.075	85.82	85.71	90.29	0.097
	Gemini-3-Pro <sup>13</sup>	88.36	0.062	83.1	88.19	93.52	0.072
	Qwen3-VL-30B-A3B Bai et al. (2025a)	83.61	0.056	79.4	77.04	81.94	0.081
	Qwen3-VL-235B-A22B Bai et al. (2025a)	89.15	0.069	88.14	86.21	90.55	0.068
	Qwen3-Omni (Base) Xu et al. (2025b)	74.84	0.137	64.0	74.21	77.68	0.117
Qwen3.5-397b-a17b <sup>16</sup>	88.34	0.055	87.6	82.93	88.70	0.080	
Specialized MLLMs	Dolphin Feng et al. (2025)	74.67	0.125	67.85	68.70	77.77	0.124
	OCRFlux <sup>7</sup>	74.82	0.193	68.03	75.75	80.23	0.202
	Mistral OCR <sup>10</sup>	78.83	0.164	82.84	70.03	78.04	0.144
	POINTS-Reader Liu et al. (2025b)	80.98	0.134	79.20	77.13	81.66	0.145
	Dolphin-1.5 Feng et al. (2025)	83.21	0.092	80.78	78.06	84.10	0.080
	olmOCR Poznanski et al. (2025)	81.79	0.096	86.04	68.92	74.77	0.121
	MinerU2-VLM Wang et al. (2024a)	85.56	0.078	80.95	83.54	87.66	0.086
	Nanonets-OCR-s Mandal et al. (2025)	85.59	0.093	85.90	80.14	85.57	0.108
	MonkeyOCR-pro-1.2B Li et al. (2025)	86.96	0.084	85.02	84.24	89.02	0.130
	Deepseek-OCR Wei et al. (2025)	87.01	0.073	83.37	84.97	88.80	0.086
	MonkeyOCR-3B Li et al. (2025)	87.13	0.075	87.45	81.39	85.92	0.129
	dots.ocr <sup>6</sup>	88.41	0.048	83.22	86.78	90.62	0.053
	OCRVerse <sup>11</sup>	88.56	0.058	86.91	84.55	88.45	0.071
	MonkeyOCR-pro-3B Li et al. (2025)	88.85	0.075	87.25	86.78	90.63	0.128
	MinerU2.5 Niu et al. (2025)	90.67	<u>0.047</u>	88.46	88.22	92.38	<u>0.044</u>
PaddleOCR-VL Cui et al. (2025a)	<b>92.86</b>	<b>0.035</b>	<u>91.22</u>	<u>90.89</u>	<b>94.76</b>	<b>0.043</b>	
General MLLMs	<b>Logics-Parsing-Omni (Ours)</b>	<u>92.54</u>	<u>0.047</u>	<b>91.3</b>	<b>91.02</b>	<u>94.31</u>	0.056

Note: Bold text indicates the best result, and underlined text indicates the second-best result.

*Result Analysis.* The experimental results of our model are presented in Table. 10. Our Logics-Parsing-Omni model performs only slightly inferior to the light-weight specialized VLM PaddleOCR-VL Cui et al. (2025a) on the overall scores, while outperforming all other models with general or specialized document-parsing capabilities. As a two-stage pipeline which separates layout analysis from element recognition, PaddleOCR-VL can perform the fine-grained optimization of the element recognition stage with a smaller and more efficient network. In contrast, Logics-Parsing-Omni integrates both layout analysis and element recognition into a unified single-stage framework. Moreover, it is designed as a general-purpose model capable of handling parsing tasks across diverse modalities, including text, images, video, and audio, which imposes significantly larger challenges for the whole model design and optimization. Despite this, Logics-Parsing-Omni still achieves the best scores on formula and table recognition, and only slightly inferior on text edit distance and table TEDS-S metric, which provides strong evidence on the effectiveness of our omni model architecture, as well as its data construction and training strategy.

### 3.3 ADVANCED MULTI-IMAGE ANALYSIS

#### 3.3.1 NATURAL IMAGE

To comprehensively evaluate the model’s performance in image difference recognition and localization, we curated a test set of 500 samples from the dataset described in Section 2.2.1. This test

set ensures diversity in scene coverage and a balanced distribution of difference operation types. To achieve fine-grained evaluation, we assess the model across two dimensions:

- **Difference Perception:** Precision and Recall are calculated based on the Intersection over Union (IoU) between predicted and ground truth bounding boxes, subject to a predefined threshold.
- **Difference Cognition:** To quantify discrepancies between predicted and reference descriptions more precisely, we employ an *LLM-as-a-Judge* mechanism. Specifically, both predicted and reference captions are parsed into lists of difference points. Precision and Recall are then computed by matching these lists. Furthermore, predicted difference points that cannot be matched to reference points due to semantic variations are categorized as *irrelevant items*, enabling the calculation of an *Irrelevance Rate* to comprehensively reflect generation quality.

*Result Analysis.* Experimental results presented in Table 11 indicate that our model significantly outperforms Qwen3-Omni-30B-A3B across both evaluation dimensions, particularly in the difference localization task. Moreover, our model’s precision surpasses that of current state-of-the-art (SOTA) commercial closed-source models, such as Gemini-3-Pro. As shown in Figure 7, our model successfully detects inter-image differences and accurately localizes these regions using bounding boxes, highlighting its robust performance in image difference tasks.

Table 11: Evaluation results on the Natural-Image Difference Module of OmniParsingBench

Model	Perception		Cognition		
	Precision (↑)	Recall (↑)	Precision (↑)	Irre. (↓)	Recall (↑)
Gemini-3-Pro	0.417	0.349	0.573	0.331	0.460
GPT-5.2	0.123	0.169	<b>0.671</b>	0.414	0.490
Qwen3.5-397B-A17B	0.383	0.328	0.621	0.376	0.461
Qwen3-VL-235B-A22B	0.356	0.293	0.653	0.339	<b>0.518</b>
Qwen3-VL-30B-A3B	0.242	0.315	0.496	0.402	0.365
Qwen3-Omni-30B-A3B	0.213	0.327	0.435	0.365	0.317
Logics-Parsing-Omni(Ours)	<b>0.689</b>	<b>0.533</b>	0.609	<b>0.180</b>	0.489

**Prompt:** 生成从第一张图编辑到第二张图的结构化解析结果。逐项列出所有变化元素，并给出对应的边界框、标签、属性及描述等信息；最后给出全局编辑描述总结整体变化。以JSON格式输出。

**Input Images:** 

**Logics-Parsing-Omni Bbox Visualization:** 

**Logics-Parsing-Omni:**

```
[{"category": "entity", "bbox": {"source": [236, 56, 466, 752], "target": null}, "tags": ["1": "人造物体", "2": "家具家居", "3": "台灯"], "attributes": {"颜色": "黑色", "位置": "书桌左侧", "类型": "可调节臂式"}, "change_tag": "Removal", "caption": "一盏黑色的可调节臂式台灯在图1中位于书桌左侧, 但在图2中被移除。"}, {"category": "entity", "bbox": {"source": null, "target": [357, 23, 389, 107]}, "tags": ["1": "人造物体", "2": "装饰品", "3": "花瓶"], "attributes": {"颜色": "蓝色", "位置": "书架顶层左侧", "材质": "陶瓷"}, "change_tag": "Addition", "caption": "一个蓝色的花瓶在图2中被新增到书架的顶层左侧, 该位置在图1中是空的。"}, {"category": "entity", "bbox": {"source": [475, 565, 560, 619], "target": [477, 563, 563, 630]}, "tags": ["1": "人造物体", "2": "文具与工具", "3": "笔记本"], "attributes": {"封面颜色": "红色", "位置": "办公椅坐垫上"}, "change_tag": "Modification", "caption": "放置在办公椅坐垫上的笔记本发生了变化: 在图1中是一个浅色封面的笔记本, 而在图2中被替换为一个红色封面的笔记本。"}, {"category": "entity", "bbox": {"source": null, "target": [350, 798, 748, 999]}, "tags": ["1": "人造物体", "2": "家具家居", "3": "地毯"], "attributes": {"颜色": "蓝色", "图案": "几何花纹", "位置": "办公椅下方"}, "change_tag": "Addition", "caption": "一块带有蓝色几何图案的地毯在图2中被新增到办公椅下方, 该地毯在图1中不存在。"}, {"category": "global", "caption": "1. 在图1中, 书桌左侧放置了一盏黑色的可调节臂式台灯, 而在图2中该台灯被移除了。2. 在图2中, 书架的顶层左侧新增了一个蓝色的花瓶, 该花瓶在图1中不存在。3. 在图1中, 办公椅的坐垫上放着一本浅色封面的笔记本, 而在图2中, 这本笔记本被替换为一本红色封面的笔记本。4. 在图2中, 办公椅下方新增了一块带有蓝色几何图案的地毯, 该地毯在图1中不存在。", "tag": "室内场景"]
```

Figure 7: Qualitative examples illustrating the natural image difference parsing capability of Logics-Parsing-Omni.

### 3.3.2 GRAPHICS

To evaluate a model’s ability to perceive fine-grained visual differences and articulate precise editing steps, we introduce the Geo-Image Difference Module of OmniParsingBench. This benchmark assesses the model’s performance on a dual-objective task: generating structured Plotting data (coordinates and relations) and Global natural language instructions.

The dataset comprises 1000 human-calibrated image pairs. We establish a hierarchical evaluation framework, as detailed in Table 12, comprising two primary dimensions: Factual Perception and Semantic Cognition.

- **Perception.** Focuses on visual grounding precision. This includes **Difference Detection** (numerical precision of coordinates and radii) and **Difference Identification** (existence of primitives and recognition of geometric/quantitative relations).
- **Cognition.** Assesses the reasoning quality of instructions. It consists of **Accuracy** (correct entity naming and geometric verbs) and **Plausibility** (logical completeness, sequence dependency, and absence of hallucinations).

Table 12: Evaluation results on the Geo-Image Difference Module of OmniParsingBench.

Model	Overall	Perception							Cognition			
		Diff Detection		Diff Identification				Accuracy		Plausibility		
		Positioning		Existence		Relation		Object	Operation	Logic	Halluc.	
		Coord.	Radius	Point	Line/Arc	Circle	Geo.					Quant.
Gemini-3-Pro	27.35	26.45	0.00	32.23	1.05	1.59	4.71	2.71	37.16	33.92	34.74	37.42
GPT-5.2	36.43	7.46	0.47	58.55	9.02	18.98	6.18	5.76	50.16	43.74	46.98	47.94
Qwen3.5-397B-A17B	33.68	11.92	0.87	44.54	2.60	6.54	6.34	4.94	46.84	43.22	44.62	45.88
Qwen3-VL-235B-A22B	32.66	13.43	0.78	59.21	5.39	18.86	4.89	4.34	42.28	36.36	39.12	41.48
Qwen3-VL-30B-A3B	29.46	36.23	1.08	57.83	5.78	14.31	2.49	2.10	33.30	29.10	31.44	34.64
Qwen3-Omni-30B-A3B	31.24	22.91	5.94	58.98	4.30	34.57	4.17	3.60	36.56	31.70	34.20	37.52
Logics-Parsing-Omni(Ours)	<b>52.81</b>	<b>43.25</b>	<b>20.28</b>	<b>69.24</b>	<b>13.30</b>	<b>63.70</b>	<b>22.04</b>	<b>12.12</b>	<b>63.60</b>	<b>59.32</b>	<b>60.52</b>	<b>68.18</b>

*Result Analysis.* As shown in Table 12, Logics-Parsing-Omni achieves an overall score of 52.81, significantly outperforming the baseline Qwen3-Omni-30B-A3B (31.24). Our model demonstrates superior performance across both perception and cognition metrics, particularly in high-precision tasks like coordinate positioning and geometric relation identification. As shown in Figure 8, Our model has achieved highly precise parsing and captioning capabilities on geometric difference diagrams, accurately locating the points of difference, describing the newly added geometric/quantitative relationships, and providing precise summarizations in natural language.

## 4 DISCUSSION

Table 13: Ablation results on the Graphics Cognition.

Model	Overall	Chart				Geometry			
		OCR & Data	Visual Elements	Logical Reasoning	Avg.	Basic Elements	Geometric Relations	Quantitative Relations	Avg.
Qwen3-Omni-30B-A3B	79.50	82.33	86.51	73.97	81.40	80.10	70.82	83.33	77.60
+ Graphics (Caption Only)	79.45	81.80	87.91	68.04	80.10	82.47	71.15	80.39	78.80
+ Graphics (Parsing & Caption)	<b>92.15</b>	<b>97.17</b>	<b>95.81</b>	<b>90.87</b>	<b>95.50</b>	<b>90.73</b>	<b>82.62</b>	<b>96.08</b>	<b>88.80</b>

To deeply validate the synergistic effectiveness between fine-grained structural parsing (Perception) and high-level semantic reasoning (Cognition), we conducted comprehensive ablation studies. The ablation models in this section are fine-tuned exclusively on our curated information-centric graphics corpus. We initialized our experiments from the zero-shot baseline model, Qwen3-Omni-30B-A3B. To evaluate the gains brought by structured data, we trained two variants. The first variant, **+ Graphics (Caption Only)**, was fine-tuned exclusively on global semantic descriptions, completely

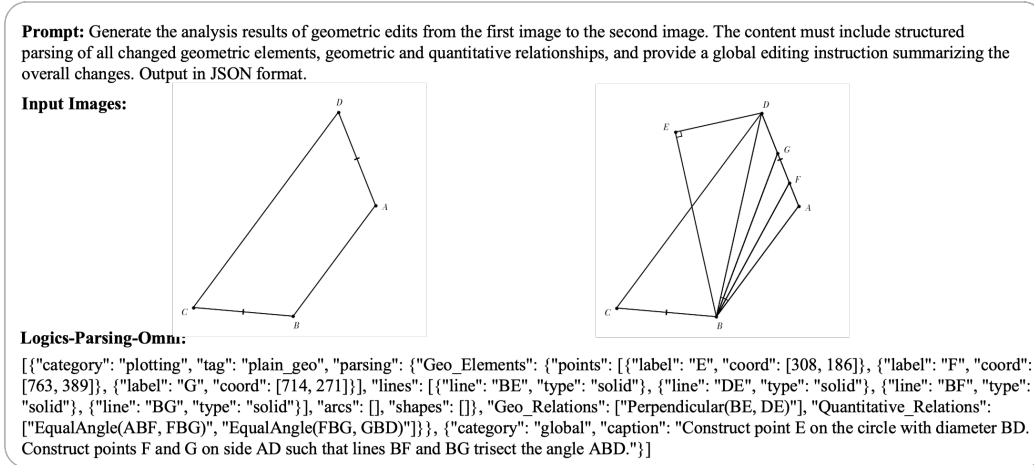


Figure 8: Qualitative examples illustrating the graphic image difference parsing capability of Logics-Parsing-Omni.

bypassing the extraction of fine-grained perception data. The second variant, **+ Graphics (Parsing & Caption)**, adopted our complete structural paradigm, which deeply integrates fine-grained perception data (eg, HTML reverse-rendering for charts, explicit topologies for geometry) with rich semantic descriptions.

Table 13 details the evaluation results on Cognition. We observe that fine-tuning solely with captions fails to improve the model, even causing a slight degradation in the overall score (from 79.50 to 79.45). Conversely, introducing the complete structured data triggers a massive performance leap, driving the overall accuracy to 92.15 (an absolute gain of 12.70 over the pure caption variant).

An analysis of the fine-grained dimensional metrics reveals that, in Chart Cognition tasks, relying solely on natural language descriptions actively harms the model’s Logical Reasoning capability, causing it to drop from 73.97 to 68.04. However, when the model is forced to learn fine-grained structural information (the Parsing & Caption variant), this metric surges to 90.87 (an absolute increase of 22.83). This proves that explicit structured anchors are crucial in helping the model perform reliable logical reasoning over implicit quantitative trends.

In the geometric domain, pure caption training similarly leads to a degradation in the Quantitative Relations metric (dropping from 83.33 to 80.39). This decline suggests that feeding the model free-form spatial descriptions without foundational anchors actually disrupts its perception of metric constraints. Conversely, introducing explicit structural parsing (which strictly defines primitive topologies and coordinates) not only rectifies this confusion—elevating Geometric Relations to 82.62—but also substantially boosts the extraction precision of Quantitative Relations to 96.08.

The aforementioned ablation results demonstrate that translating abstract visual signals into enumerable, structurally faithful fine-grained perception data serves as an indispensable foundation for achieving reliable, high-level semantic cognition.

## 5 CONCLUSIONS

In this paper, we presented Logics-Parsing-Omni, a unified multimodal framework that effectively bridges the chasm between pixel-level perception and semantic cognition. By implementing the Omni Parsing paradigm—supported by a meticulously curated standardized corpus and a two-stage progressive training strategy—we have successfully transformed unstructured heterogeneous data (spanning documents, images, and audio-visual streams) into locatable, enumerable, and traceable knowledge. Empirical results on OmniParsingBench confirm that our model not only achieves state-of-the-art performance across diverse modalities but also validates the synergy between fine-grained structural fidelity and deep logical reasoning. Moving forward, we aim to further advance this fron-

---

tier by optimizing computational efficiency and developing robust cross-modal continual learning mechanisms, paving the way for more scalable and adaptive knowledge-intensive AI systems.

## 6 CONTRIBUTION

The contributors' names are sorted in alphabetical order of the last name.

### **Core Contributors**

Xin An, Jingyi Cai, Xiangyang Chen, Huayao Liu, Peiting Liu, Peng Wang, Bei Yang, Xiuwen Zhu

### **Contributors**

Yongfan Chen, Baoyu Hou, Shuzhao Li, Weidong Ren, Fan Yang, Jiangtao Zhang

### **Project Leads**

Lin Qu, Xiaoxiao Xu

## REFERENCES

Abdelrahman Abdallah, Alexander Berendeyev, Islam Nuradin, and Daniyar B. Nurseitov. TNCR: table net detection and classification dataset. *CoRR*, abs/2106.15322, 2021. URL <https://arxiv.org/abs/2106.15322>.

Inclusion AI, Bowen Ma, Cheng Zou, Canxiang Yan, Chunxiang Jin, Chunjie Shen, Chenyu Lian, Dandan Zheng, Fudong Wang, Furong Xu, et al. Ming-flash-omni: A sparse, unified architecture for multimodal perception and generation. *arXiv preprint arXiv:2510.24821*, 2025.

Keyu An, Qian Chen, Chong Deng, Zhihao Du, Changfeng Gao, Zhifu Gao, Yue Gu, Ting He, Hangrui Hu, Kai Hu, et al. Funaudiollm: Voice understanding and generation foundation models for natural interaction between humans and llms. *arXiv preprint arXiv:2407.04051*, 2024.

Xiang An, Yin Xie, Kaicheng Yang, Wenkang Zhang, Xiuwei Zhao, Zheng Cheng, Yirui Wang, Songcen Xu, Changrui Chen, Chunsheng Wu, Huajie Tan, Chunyuan Li, Jing Yang, Jie Yu, Xiyao Wang, Bin Qin, Yumeng Wang, Zizhen Yan, Ziyong Feng, Ziwei Liu, Bo Li, and Jiankang Deng. Llava-onevision-1.5: Fully open framework for democratized multimodal training. In *arXiv*, 2025.

Shuai Bai, Yuxuan Cai, Ruizhe Chen, Keqin Chen, Xionghui Chen, Zesen Cheng, Lianghao Deng, Wei Ding, Chang Gao, Chunjiang Ge, Wenbin Ge, Zhifang Guo, Qidong Huang, Jie Huang, Fei Huang, Binyuan Hui, Shutong Jiang, Zhaohai Li, Mingsheng Li, Mei Li, Kaixin Li, Zicheng Lin, Junyang Lin, Xuejing Liu, Jiawei Liu, Chenglong Liu, Yang Liu, Dayiheng Liu, Shixuan Liu, Dunjie Lu, Ruilin Luo, Chenxu Lv, Rui Men, Lingchen Meng, Xuancheng Ren, Xingzhang Ren, Sibao Song, Yuchong Sun, Jun Tang, Jianhong Tu, Jianqiang Wan, Peng Wang, Pengfei Wang, Qiyue Wang, Yuxuan Wang, Tianbao Xie, Yiheng Xu, Haiyang Xu, Jin Xu, Zhibo Yang, Mingkun Yang, Jianxin Yang, An Yang, Bowen Yu, Fei Zhang, Hang Zhang, Xi Zhang, Bo Zheng, Humen Zhong, Jingren Zhou, Fan Zhou, Jing Zhou, Yuanzhi Zhu, and Ke Zhu. Qwen3-vl technical report. *arXiv preprint arXiv:2511.21631*, 2025a.

Shuai Bai, Keqin Chen, Xuejing Liu, Jialin Wang, Wenbin Ge, Sibao Song, Kai Dang, Peng Wang, Shijie Wang, Jun Tang, et al. Qwen2. 5-vl technical report. *arXiv preprint arXiv:2502.13923*, 2025b.

Pengfei Cai, Yan Song, Qing Gu, Nan Jiang, Haoyu Song, and Ian McLoughlin. Detect any sound: Open-vocabulary sound event detection with multi-modal queries, 2025. URL <https://arxiv.org/abs/2507.16343>.

Xiangyang Chen, Shuzhao Li, Xiuwen Zhu, Yongfan Chen, Fan Yang, Cheng Fang, Lin Qu, Xiaoxiao Xu, Hu Wei, and Minggang Wu. Logics-parsing technical report. *arXiv preprint arXiv:2509.19760*, 2025.

- 
- Gheorghe Comanici, Eric Bieber, Mike Schaekermann, Ice Pasupat, Noveen Sachdeva, Inderjit Dhillon, Marcel Blistein, Ori Ram, Dan Zhang, Evan Rosen, et al. Gemini 2.5: Pushing the frontier with advanced reasoning, multimodality, long context, and next generation agentic capabilities. *arXiv preprint arXiv:2507.06261*, 2025.
- Cheng Cui, Ting Sun, Suyin Liang, Tingquan Gao, Zelun Zhang, Jiaxuan Liu, Xueqing Wang, Changda Zhou, Hongen Liu, Manhui Lin, Yue Zhang, Yubo Zhang, Handong Zheng, Jing Zhang, Jun Zhang, Yi Liu, Dianhai Yu, and Yanjun Ma. Paddleocr-vl: Boosting multilingual document parsing via a 0.9b ultra-compact vision-language model, 2025a. URL <https://arxiv.org/abs/2510.14528>.
- Cheng Cui, Ting Sun, Manhui Lin, Tingquan Gao, Yubo Zhang, Jiaxuan Liu, Xueqing Wang, Zelun Zhang, Changda Zhou, Hongen Liu, Yue Zhang, Wenyu Lv, Kui Huang, Yichao Zhang, Jing Zhang, Jun Zhang, Yi Liu, Dianhai Yu, and Yanjun Ma. Paddleocr 3.0 technical report, 2025b. URL <https://arxiv.org/abs/2507.05595>.
- Cheng Cui, Ting Sun, Manhui Lin, Tingquan Gao, Yubo Zhang, Jiaxuan Liu, Xueqing Wang, Zelun Zhang, Changda Zhou, Hongen Liu, et al. Paddleocr 3.0 technical report. *arXiv preprint arXiv:2507.05595*, 2025c.
- Cheng Cui, Ting Sun, Suyin Liang, Tingquan Gao, Zelun Zhang, Jiaxuan Liu, Xueqing Wang, Changda Zhou, Hongen Liu, Manhui Lin, et al. Paddleocr-vl-1.5: Towards a multi-task 0.9 b vlm for robust in-the-wild document parsing. *arXiv preprint arXiv:2601.21957*, 2026.
- Pritam Deka. mermaid-diagrams-flat-original [dataset]. <https://huggingface.co/datasets/pritamdeka/mermaid-diagrams-flat-original>, 2025. Accessed: 2025-12-10.
- Hao Feng, Shu Wei, Xiang Fei, Wei Shi, Yingdong Han, Lei Liao, Jinghui Lu, Binghong Wu, Qi Liu, Chunhui Lin, et al. Dolphin: Document image parsing via heterogeneous anchor prompting. *arXiv preprint arXiv:2505.14059*, 2025.
- Shawn Hershey, Daniel P W Ellis, Eduardo Fonseca, Aren Jansen, Caroline Liu, R Channing Moore, and Manoj Plakal. The benefit of temporally-strong labels in audio event classification, 2021. URL <https://arxiv.org/abs/2105.07031>.
- Jack Hong, Shilin Yan, Jiayin Cai, Xiaolong Jiang, Yao Hu, and Weidi Xie. Worldsense: Evaluating real-world omnimodal understanding for multimodal llms. *arXiv preprint arXiv:2502.04326*, 2025.
- Horizon Team, MiLM Plus. Midashenglm: Efficient audio understanding with general audio captions. Technical report, Xiaomi Inc., 2025. URL <https://arxiv.org/abs/2508.03983>. Contributors: Heinrich Dinkel et al. (listed alphabetically in Appendix B).
- Anwen Hu, Haiyang Xu, Jiabo Ye, Ming Yan, Liang Zhang, Bo Zhang, Ji Zhang, Qin Jin, Fei Huang, and Jingren Zhou. mplug-docowl 1.5: Unified structure learning for ocr-free document understanding. In *Findings of the Association for Computational Linguistics: EMNLP 2024*, pp. 3096–3120, 2024.
- Qingqiu Huang, Yu Xiong, Anyi Rao, Jiase Wang, and Dahua Lin. Movienet: A holistic dataset for movie understanding. In *European conference on computer vision*, pp. 709–727. Springer, 2020.
- Bo Li, Yuanhan Zhang, Dong Guo, Renrui Zhang, Feng Li, Hao Zhang, Kaichen Zhang, Peiyuan Zhang, Yanwei Li, Ziwei Liu, et al. Llava-onevision: Easy visual task transfer. *arXiv preprint arXiv:2408.03326*, 2024.
- Zhang Li, Yuliang Liu, Qiang Liu, Zhiyin Ma, Ziyang Zhang, Shuo Zhang, Zidun Guo, Jiarui Zhang, Xinyu Wang, and Xiang Bai. Monkeyocr: Document parsing with a structure-recognition-relation triplet paradigm, 2025. URL <https://arxiv.org/abs/2506.05218>.
- Zhiqiu Lin, Siyuan Cen, Daniel Jiang, Jay Karhade, Hewei Wang, Chancharik Mitra, Tiffany Ling, Yuhan Huang, Sifan Liu, Mingyu Chen, et al. Towards understanding camera motions in any video. *arXiv preprint arXiv:2504.15376*, 2025.

- 
- Haotian Liu, Chunyuan Li, Qingyang Wu, and Yong Jae Lee. Visual instruction tuning, 2023.
- Pengfei Liu, Jun Tao, and Zhixiang Ren. A quantitative analysis of knowledge-learning preferences in large language models in molecular science, 2025a. URL <https://arxiv.org/abs/2402.04119>.
- Yuan Liu, Zhongyin Zhao, Le Tian, Haicheng Wang, Xubing Ye, Yangxiu You, Zilin Yu, Chuhan Wu, Zhou Xiao, Yang Yu, et al. Points-reader: Distillation-free adaptation of vision-language models for document conversion. In *Proceedings of the 2025 Conference on Empirical Methods in Natural Language Processing*, pp. 1576–1601, 2025b.
- Kingsoft LLM. Qzhou-flowchart-qa [dataset]. <https://huggingface.co/datasets/Kingsoft-LLM/QZhou-Flowchart-QA>, 2025. Accessed: 2025-12-10.
- Souvik Mandal, Ashish Talewar, Paras Ahuja, and Prathamesh Juvatkar. Nanonets-ocr-s: A model for transforming documents into structured markdown with intelligent content recognition and semantic tagging, 2025.
- Junbo Niu, Zheng Liu, Zhuangcheng Gu, Bin Wang, Linke Ouyang, Zhiyuan Zhao, Tao Chu, Tianyao He, Fan Wu, Qintong Zhang, et al. Mineru2. 5: A decoupled vision-language model for efficient high-resolution document parsing. *arXiv preprint arXiv:2509.22186*, 2025.
- Vassil Panayotov, Guoguo Chen, Daniel Povey, and Sanjeev Khudanpur. Librispeech: an asr corpus based on public domain audio books. In *Acoustics, Speech and Signal Processing (ICASSP), 2015 IEEE International Conference on*, pp. 5206–5210. IEEE, 2015.
- Shuai Peng, Di Fu, Liangcai Gao, Xiuqin Zhong, Hongguang Fu, and Zhi Tang. Multi-math: Bridging visual and mathematical reasoning for large language models. *arXiv preprint arXiv:2409.00147*, 2024.
- Jake Poznanski, Aman Rangapur, Jon Borchardt, Jason Dunkelberger, Regan Huff, Daniel Lin, Christopher Wilhelm, Kyle Lo, and Luca Soldaini. olmocr: Unlocking trillions of tokens in pdfs with vision language models. *arXiv preprint arXiv:2502.18443*, 2025.
- Alec Radford, Jong Wook Kim, Tao Xu, Greg Brockman, Christine McLeavey, and Ilya Sutskever. Robust speech recognition via large-scale weak supervision, 2022. URL <https://arxiv.org/abs/2212.04356>.
- Stephan Roecker. mermaid-flowchart-transformer-moondream-caption [dataset]. <https://huggingface.co/datasets/sroecker/mermaid-flowchart-transformer-moondream-caption>, 2024. Accessed: 2025-12-10.
- tbt0205. flowchart4 [dataset]. <https://huggingface.co/datasets/tbt0205/flowchart4>, 2025. Accessed: 2025-12-10.
- Hunyuan Vision Team, Pengyuan Lyu, Xingyu Wan, Gengluo Li, Shangpin Peng, Weinong Wang, Liang Wu, Huawei Shen, Yu Zhou, Canhui Tang, et al. Hunyuanocr technical report. *arXiv preprint arXiv:2511.19575*, 2025a.
- Meituan LongCat Team, Bairui Wang, Bin Xiao, Bo Zhang, Bolin Rong, Borun Chen, Chang Wan, Chao Zhang, Chen Huang, Chen Chen, et al. Longcat-flash-omni technical report. *arXiv preprint arXiv:2511.00279*, 2025b.
- Bin Wang, Chao Xu, Xiaomeng Zhao, Linke Ouyang, Fan Wu, Zhiyuan Zhao, Rui Xu, Kaiwen Liu, Yuan Qu, Fukai Shang, et al. Mineru: An open-source solution for precise document content extraction. *arXiv preprint arXiv:2409.18839*, 2024a.
- Bin Wang, Fan Wu, Linke Ouyang, Zhuangcheng Gu, Rui Zhang, Renqiu Xia, Botian Shi, Bo Zhang, and Conghui He. Image over text: Transforming formula recognition evaluation with character detection matching. In *Proceedings of the Computer Vision and Pattern Recognition Conference*, pp. 19681–19690, 2025a.

- 
- Hui Wang, Siqi Zheng, Yafeng Chen, Luyao Cheng, and Qian Chen. Cam++: A fast and efficient network for speaker verification using context-aware masking, 2023. URL <https://arxiv.org/abs/2303.00332>.
- Jianyuan Wang, Minghao Chen, Nikita Karaev, Andrea Vedaldi, Christian Rupprecht, and David Novotny. Vggt: Visual geometry grounded transformer. In *Proceedings of the Computer Vision and Pattern Recognition Conference*, pp. 5294–5306, 2025b.
- Peng Wang, Shuai Bai, Sinan Tan, Shijie Wang, Zhihao Fan, Jinze Bai, Keqin Chen, Xuejing Liu, Jialin Wang, Wenbin Ge, et al. Qwen2-vl: Enhancing vision-language model’s perception of the world at any resolution. *arXiv preprint arXiv:2409.12191*, 2024b.
- Weiyun Wang, Zhangwei Gao, Lixin Gu, Hengjun Pu, Long Cui, Xingguang Wei, Zhaoyang Liu, Linglin Jing, Shenglong Ye, Jie Shao, et al. Internvl3. 5: Advancing open-source multimodal models in versatility, reasoning, and efficiency. *arXiv preprint arXiv:2508.18265*, 2025c.
- Haoran Wei, Chenglong Liu, Jinyue Chen, Jia Wang, Lingyu Kong, Yanming Xu, Zheng Ge, Liang Zhao, Jianjian Sun, Yuang Peng, et al. General ocr theory: Towards ocr-2.0 via a unified end-to-end model. *arXiv preprint arXiv:2409.01704*, 2024.
- Haoran Wei, Yaofeng Sun, and Yukun Li. Deepseek-ocr: Contexts optical compression. *arXiv preprint arXiv:2510.18234*, 2025.
- Haoran Wei, Yaofeng Sun, and Yukun Li. Deepseek-ocr 2: Visual causal flow. *arXiv preprint arXiv:2601.20552*, 2026.
- Jin Xu, Zhifang Guo, Jinzheng He, Hangrui Hu, Ting He, Shuai Bai, Keqin Chen, Jialin Wang, Yang Fan, Kai Dang, et al. Qwen2. 5-omni technical report. *arXiv preprint arXiv:2503.20215*, 2025a.
- Jin Xu, Zhifang Guo, Hangrui Hu, Yunfei Chu, Xiong Wang, Jinzheng He, Yuxuan Wang, Xian Shi, Ting He, Xinfu Zhu, Yuanjun Lv, Yongqi Wang, Dake Guo, He Wang, Linhan Ma, Pei Zhang, Xinyu Zhang, Hongkun Hao, Zishan Guo, Baosong Yang, Bin Zhang, Ziyang Ma, Xipin Wei, Shuai Bai, Keqin Chen, Xuejing Liu, Peng Wang, Mingkun Yang, Dayiheng Liu, Xingzhang Ren, Bo Zheng, Rui Men, Fan Zhou, Bowen Yu, Jianxin Yang, Le Yu, Jingren Zhou, and Junyang Lin. Qwen3-omni technical report. *arXiv preprint arXiv:2509.17765*, 2025b.
- Kai-Tuo Xu, Feng-Long Xie, Xu Tang, and Yao Hu. Fireredasr: Open-source industrial-grade mandarin speech recognition models from encoder-decoder to llm integration, 2025c. URL <https://arxiv.org/abs/2501.14350>.
- Yan Yang, Haochen Tian, Yang Shi, Wulin Xie, Yi-Fan Zhang, Yuhao Dong, Yiibo Hu, Liang Wang, Ran He, Caifeng Shan, et al. A survey of unified multimodal understanding and generation: Advances and challenges. *Authorea Preprints*, 2025.
- Wenqi Zhang, Hang Zhang, Xin Li, Jiashuo Sun, Yongliang Shen, Weiming Lu, Deli Zhao, Yueting Zhuang, and Lidong Bing. 2.5 years in class: A multimodal textbook for vision-language pretraining. *arXiv preprint arXiv:2501.00958*, 2025.
- Yuze Zhao, Jintao Huang, Jinghan Hu, Xingjun Wang, Yunlin Mao, Daoze Zhang, Zeyinzi Jiang, Zhikai Wu, Baole Ai, Ang Wang, Wenmeng Zhou, and Yingda Chen. Swift:a scalable lightweight infrastructure for fine-tuning, 2024. URL <https://arxiv.org/abs/2408.05517>.
- Xinyi Zheng, Douglas Burdick, Lucian Popa, and Nancy Xin Ru Wang. Global table extractor (GTE): A framework for joint table identification and cell structure recognition using visual context. *CoRR*, abs/2005.00589, 2020. URL <https://arxiv.org/abs/2005.00589>.
- Xu Zhong, Elaheh ShafieiBavani, and Antonio Jimeno-Yepes. Image-based table recognition: data, model, and evaluation. *CoRR*, abs/1911.10683, 2019. URL <http://arxiv.org/abs/1911.10683>.
- Jinguo Zhu, Weiyun Wang, Zhe Chen, Zhaoyang Liu, Shenglong Ye, Lixin Gu, Hao Tian, Yuchen Duan, Weijie Su, Jie Shao, et al. Internvl3: Exploring advanced training and test-time recipes for open-source multimodal models. *arXiv preprint arXiv:2504.10479*, 2025.

## A APPENDIX

### A.1 DETAILED EVALUATION ON THE NATURAL IMAGE MODULE OF OMNIPARSINGBENCH

**Perception Analysis.** Perception metrics compute instance-level parsing score: an entity or text instance is counted correct *only if* (1) its bounding box achieves IoU  $\geq 0.5$  with ground truth, *and* (2) all semantic/text fields pass verification (LLM-verified semantic consistency for entities; exact string match for OCR (edit distance score over 0.75 as match), language in text).  $Score = \frac{\text{correctly parsed instances}}{\text{total ground truth instances}}$ . As shown in Table 14, Logics-Parsing-Omni advances fine-grained structural parsing through balanced gains in localization capability and semantic fidelity, enabling more precise scene decomposition.

However, knowledge-aware entity parsing remains a key challenge: despite strong localization recall (70.44%), semantic accuracy drops to 59.81% due to difficulties in precisely referencing verified knowledge identifiers. This gap highlights the need for targeted strategies—such as knowledge-grounded data synthesis, contrastive identifier training, external knowledge retrieval integration—to strengthen factual grounding without compromising structural parsing integrity.

Table 14: Detailed Evaluation Results on the Natural Image module of OmniParsingBench - Perception

Model	Entity			Knowledge-Aware Entity			Text			Average	
	Loc. Recall	Sem. Acc.*	Score	Loc. Recall	Sem. Acc.*	Score	Loc. Recall	OCR Acc.*	Lang. Acc.*		Score
Gemini 3 Pro	<b>82.43</b>	<b>98.64</b>	<b>81.32</b>	66.44	75.69	<b>50.29</b>	<b>86.12</b>	<b>74.39</b>	88.59	57.84	<b>63.15</b>
GPT 5.2 <sup>†</sup>	61.98	95.11	58.95	-	-	-	70.32	46.36	82.76	28.60	46.07
Qwen3.5-397B-A17B	57.83	97.42	56.33	53.79	<b>80.41</b>	43.25	79.51	62.21	83.51	41.78	47.12
Qwen3-VL-235B-A22B-Instruct	58.33	97.85	57.08	66.00	68.61	45.28	81.65	67.32	89.61	60.63	50.62
Qwen3-VL-30B-A3B-Instruct	52.97	97.51	51.66	63.28	57.37	36.30	86.31	67.94	85.71	51.45	46.47
Qwen3-Omni-30B-A3B-Instruct (base)	57.96	97.92	56.75	41.30	57.26	23.65	75.65	71.40	83.63	45.45	41.95
<b>Logics Parsing Omni (ours)</b>	65.14	97.88	63.75	<b>70.44</b>	59.81	42.13	73.17	66.56	<b>91.90</b>	<b>62.49</b>	50.53

\* Sem. Acc., OCR Acc. and Lang. Acc. are computed conditionally on successfully localized instances. Localization Recall and final Score metrics use total instances as denominator.

<sup>†</sup> Note that GPT seems to fail to identify some knowledge-aware entities due to its model strategy, knowledge metrics are ignored here.

**Cognition Analysis.** Cognition metrics evaluate global caption quality via two components: (1) *Caption QA Accuracy*: Human-annotated question sets aligned with nine semantic aspects (theme, emotion, scene, etc.) are answered by an LLM using *only* the model-generated caption; per-aspect accuracy is macro-averaged across images. (2) *Knowledge Mention Accuracy*: Proportion of knowledge-annotated images where the caption explicitly and correctly references *all* verified knowledge entities (LLM-verified).

Table 15 presents detailed evaluation results on cognition Caption QA. The *Answerable* metric quantifies caption comprehensiveness (proportion of QA pairs addressable by the caption), while *Precision* reflects factual accuracy of answered questions—serving as a direct indicator of hallucination control. Logics Parsing Omni achieves leading performance across all semantic aspects in parsing-derived caption evaluation, with the highest Answerable rate and robust Precision among open-weight models, demonstrating an optimal balance between informational coverage and semantic fidelity.

A critical observation is that parsing-derived captions from most models are significantly shorter than their direct dense captions (e.g., Gemini-3-Pro: 418 vs. 600 tokens; Qwen3-Omni-30B-A3B: 258 vs. 490 tokens), potentially introducing length-related bias in caption quality assessment. To ensure a fair and length-agnostic comparison, we additionally evaluate all models’ direct dense captioning capability under identical QA protocols. The results confirm that Logics-Parsing-Omni maintains clear leadership: its parsing-generated caption achieves a 90.36% overall QA score—surpassing all open-weight baselines’ dense captions and approaching Gemini-3-Pro’s dense caption performance (94.15%). This demonstrates that knowledge-enhanced structured parsing inherently produces captions with superior semantic density and factual reliability, without relying on verbose generation. The framework effectively decouples caption quality from length, validating its robustness for high-fidelity visual cognition.

#### Limitations and Future Directions.

*Benchmark Design.* Fig. 9 shows 2 image parsing results from Logics-Parsing-Omni sampled from the Natural Image module of OmniParsingBench. Current evaluation faces two inherent constraints: (1) Localization recall for entities and text is sensitive to annotation ambiguities—such as whether

Table 15: Detailed Evaluation Results on the Natural Image module of OmniParsingBench - Cognition.

Model	Overall Metrics			Caption Length	Detailed Evaluation Metrics								
	Overall	Answerable	Precision		Theme	Emotion	Scene	Count	Attribute	Location	Text	Style	Composition
<i>Direct Dense Caption</i>													
Gemini 3 Pro	<b>94.15</b>	<b>97.21</b>	<b>96.86</b>	<b>600</b>	<b>99.77</b>	<b>99.48</b>	<b>98.45</b>	<b>83.81</b>	<b>95.93</b>	<b>90.90</b>	<b>96.08</b>	<b>98.23</b>	<b>93.39</b>
GPT 5.2	86.06	90.94	94.63	824	94.88	73.12	93.05	74.55	85.76	85.38	74.34	95.70	91.22
Qwen3.5-397B-A17B	91.45	90.94	95.44	565	98.94	96.35	96.75	81.56	92.23	88.27	91.50	97.12	89.71
Qwen3-VL-235B-A22B-Instruct	86.95	92.77	93.72	504	98.95	96.35	95.83	76.28	88.03	78.07	88.89	94.69	83.38
Qwen3-VL-30B-A3B-Instruct	84.70	90.77	93.31	515	98.24	94.79	94.27	72.29	85.44	74.81	79.08	94.90	87.34
Qwen3-Omni-30B-A3B-Instruct	84.01	90.78	92.54	490	98.33	95.72	93.36	72.97	85.03	73.34	84.11	91.70	81.45
<i>Caption from Image parsing</i>													
Gemini 3 Pro	89.87	93.04	<b>96.60</b>	418	<b>99.52</b>	<b>98.95</b>	<b>96.54</b>	76.84	90.16	<b>87.26</b>	87.92	97.48	88.24
GPT 5.2	81.71	86.00	95.01	569	96.03	76.57	94.13	69.97	78.11	79.97	76.81	94.27	86.16
Qwen3.5-397B-A17B	76.46	82.73	92.43	268	97.52	90.10	90.22	64.46	72.22	68.02	73.03	92.67	77.04
Qwen3-VL-235B-A22B-Instruct	82.70	87.69	94.37	456	98.71	98.43	92.24	69.43	83.20	72.90	81.45	94.67	78.10
Qwen3-VL-30B-A3B-Instruct	75.68	81.47	92.90	320	98.70	94.14	90.63	63.43	74.75	58.57	67.11	90.85	76.20
Qwen3-Omni-30B-A3B-Instruct	74.34	79.84	93.11	258	98.09	93.18	90.02	61.57	72.39	59.67	65.47	90.26	72.25
<b>Logics Parsing Omni (Ours)</b>	<b>90.36</b>	<b>94.85</b>	95.27	<b>827</b>	98.82	97.40	96.27	<b>78.38</b>	<b>91.19</b>	86.11	<b>88.82</b>	<b>97.77</b>	<b>92.33</b>

closely spaced objects constitute single or multiple entities, or how fragmented/multi-line text should be segmented. These subjective boundaries may induce false negatives in matching-based evaluation, suggesting a need for uncertainty-aware metrics or soft-matching protocols in future benchmarks. (2) The framework emphasizes recall-oriented assessment but lacks explicit quantification of hallucination (i.e., spurious entity/text generation). Integrating precision-focused metrics and false-positive analysis will enable more holistic reliability evaluation.

*Model Scope.* Knowledge-aware parsing remains challenging, as reflected in moderate accuracy for knowledge entity recognition—highlighting the need for more scalable knowledge integration strategies. Furthermore, the current parsing schema prioritizes objective elements (entities, text), while higher-level semantic dimensions—such as aesthetic quality, scene narrative coherence, emotional resonance, and technical image attributes remain under-explored. Future iterations of structured parsing should expand the semantic scope to encompass these dimensions, fostering a more comprehensive understanding of visual content. These directions will guide both benchmark evolution and model development toward holistic image interpretation.

## A.2 DETAILED EVALUATION ON THE GRAPHICS MODULE OF OMNIPARSINGBENCH

As discussed in the main text, we systematically merged the evaluation metrics into Perception and Cognition dimensions to provide a macroscopic view of the model’s graphics capabilities. In this section, we present the fine-grained, deconstructed evaluation results for the Chart and Geometry domains, providing deeper insights into the specific strengths of Logics-Parsing-Omni. To clearly bridge the unified graphics results in the main text (Table 4) with the granular metrics presented below, we introduce the exact cross-domain aggregation rules as follows:

### Perception:

- **Location:** Represents geometric spatial positioning, derived from the average of coordinate and radius metrics in the Geometry domain.  

$$\text{Location} = \frac{1}{2} (\text{Geo}_{\text{Coord}} + \text{Geo}_{\text{Radius}})$$
- **Content - Element:** Evaluates the exact existence and recall of fundamental geometric elements.  

$$\text{Element} = \frac{1}{3} (\text{Geo}_{\text{Point}} + \text{Geo}_{\text{Line/Arc}} + \text{Geo}_{\text{Circle}})$$
- **Content - Relation:** Derived exclusively from explicit structural and quantitative relationships in geometry.  

$$\text{Relation} = \frac{1}{2} (\text{Geo}_{\text{Geo. Rel.}} + \text{Geo}_{\text{Quant. Rel.}})$$
- **Content - Chart:** Represents the exactness of HTML structural parsing in the Chart domain, directly adopting the structural F1-Score.  

$$\text{Chart} = \text{Chart}_{\text{Avg.}}$$
- **Avg.:** The macro-average of the four detailed perception metrics above.  

$$\text{Avg.} = \frac{1}{4} (\text{Location} + \text{Element} + \text{Relation} + \text{Chart})$$

### Cognition:

- **Element:** Represents the fundamental information extraction capability across both domains.  
 $\text{Element} = \frac{1}{2} (\text{Chart}_{\text{OCR \& Data}} + \text{Geo}_{\text{Basic Elements}})$
- **Relation:** Captures the ability to extract and bind topological and visual structures.  
 $\text{Relation} = \frac{1}{3} (\text{Chart}_{\text{Visual Elements}} + \text{Geo}_{\text{Geometric Rel.}} + \text{Geo}_{\text{Quantitative Rel.}})$
- **Reasoning:** Represents complex logical deduction via implicit chart trends.  
 $\text{Reasoning} = \text{Chart}_{\text{Logical Reasoning}}$
- **Avg.:** The exact mean of these three cognitive dimensions.  
 $\text{Avg.} = \frac{1}{3} (\text{Element} + \text{Relation} + \text{Reasoning})$

**Chart.** Table 16 details the models’ performance on the Chart sub-benchmark. The Perception phase evaluates the exactness of structural reverse-rendering across diverse visual representations. Specifically, it measures the data extraction accuracy for statistical charts (e.g., bar and line charts) using the F1-score (Stat. Charts), and assesses the topological correctness of structural diagrams (e.g., flowcharts) via sequence similarity (Struct. Diagrams). Concurrently, the Cognition phase assesses the semantic coverage and reasoning capabilities over these extracted structures.

As shown in Table 16, Logics-Parsing-Omni attains an overall score of 91.71, an absolute gain of 7.91 over the baseline (Qwen3-Omni-30B-A3B). This leap is primarily driven by its profound cognitive capabilities, where our model exhibits absolute dominance in fine-grained data comprehension and visual fact grounding. By enforcing strict structural alignment, Logics-Parsing-Omni achieves outstanding performance in both *OCR & Data* (97.88) and *Visual Elements* (95.81).

Table 16: Detailed Evaluation Results on the Graphics Module of OmniParsingBench - Chart.

Model	Overall	Perception			Cognition			
		Stat. Charts (F1)	Struct. Diagrams (Sim.)	Avg.	OCR & Data	Visual Elements	Logical Reasoning	Avg. Acc.
Gemini-3-Pro <sup>13</sup>	88.00	87.43	89.60	87.80	89.22	90.70	83.11	88.20
GPT-5.2 <sup>9</sup>	88.28	79.63	87.49	83.56	94.88	87.21	<b>93.95</b>	93.00
Qwen3.5-397B-A17B <sup>16</sup>	87.41	<b>92.28</b>	<b>90.12</b>	<b>91.91</b>	83.57	90.23	73.97	82.90
Qwen3-VL-235B-A22B Bai et al. (2025a)	86.05	84.51	81.46	83.99	89.22	91.63	81.74	88.10
Qwen3-VL-30B-A3B Bai et al. (2025a)	75.90	63.22	87.76	67.40	86.75	88.37	74.43	84.40
Qwen3-Omni-30B-A3B Xu et al. (2025b)	83.80	88.08	76.97	86.19	82.33	86.51	73.97	81.40
<b>Logics-Parsing-Omni (Ours)</b>	<b>91.71</b>	88.13	88.06	88.12	<b>97.88</b>	<b>95.81</b>	88.13	<b>95.30</b>

**Geometry.** Table 17 presents the model’s performance on the Geometry sub-benchmark. To rigorously assess the model’s capability in decoupling complex spatial topologies and mathematical constraints, the Perception phase within this specific domain employs a specialized weighted metric for its internal *Avg. Score*: exact positioning of coordinates and radii (30% weight), verifying the existence of basic elements like points, lines/arcs, and circles (30% weight), and extracting explicit relations encompassing geometric topologies and quantitative annotations (40% weight). Concurrently, the Cognition evaluation adopts a semantic-coverage QA framework designed to assess the understanding of basic elements, geometric relations (e.g., parallelism, collinearity), and quantitative relations.

For geometry, our model’s overall score improved from 71.53 to 85.98, a significant improvement primarily attributed to its fine-grained Perception layer. Logics-Parsing-Omni achieves an exceptional 82.24 in Coordinate Positioning, marking a massive leap from the baseline (32.79) and vastly outperforming Gemini-3-Pro (74.27). Anchored by this precise spatial perception, our model attains the highest average Cognition accuracy (91.90). It excels particularly in the semantic extraction of Basic Elements (94.44) and Quantitative Relations (95.10).

### A.3 DETAILED EVALUATION ON THE AUDIO MODULE OF OMNIPARSINGBENCH

The exact calculation rules of (Table 6) as follows:

#### Perception:

- **Avg.:** Aggregates the fundamental audio perception metrics, specifically Time F1, Key F1, and ASR WER.  
 $\text{Avg.} = \frac{1}{3} (\text{Time} + \text{Key} + (1 - \min(1, \text{ASR})) \times 100)$

Table 17: Detailed evaluation results on the Graphics Module of OmniParsingBench - Geometrics.

Model	Overall	Perception							Cognition				
		Positioning		Existence			Relation		Avg.	Basic Elements	Geometric Relations	Quantitative Relations	Avg.
		Coord.	Radius	Point	Line/Arc	Circle	Geo.	Quant.					
Gemini-3-Pro <sup>13</sup>	<b>87.49</b>	74.27	85.80	<b>93.64</b>	<b>70.94</b>	97.57	<b>80.72</b>	<b>91.52</b>	<b>84.67</b>	91.74	<b>94.12</b>	86.23	90.30
GPT-5.2 <sup>9</sup>	77.60	5.29	86.38	90.54	64.65	<b>97.73</b>	59.34	75.97	66.10	89.88	85.90	94.12	89.10
Qwen3.5-397B-A17B <sup>16</sup>	78.59	7.34	86.05	89.69	62.55	96.80	70.93	81.33	69.37	89.38	82.62	94.12	87.80
Qwen3-VL-235B-A22B Bai et al. (2025a)	73.92	16.68	88.95	90.70	64.41	97.40	52.38	82.85	68.14	84.15	67.54	90.20	79.70
Qwen3-VL-30B-A3B Bai et al. (2025a)	70.85	37.93	86.75	87.83	61.31	97.17	38.70	68.11	64.69	78.58	70.16	88.24	77.00
Qwen3-Omni-30B-A3B Xu et al. (2025b)	71.53	32.79	87.55	89.28	61.42	97.57	43.11	69.76	65.45	80.10	70.82	83.33	77.60
<b>Logics-Parsing-Omni (Ours)</b>	85.98	<b>82.24</b>	<b>90.35</b>	92.75	62.14	95.13	62.25	83.57	80.06	<b>94.44</b>	85.90	<b>95.10</b>	<b>91.90</b>

Table 18: Detailed evaluation results on the Natural Videos Module of OmniParsingBench - Camera.

Model	Overall	Perception			Cognition
		Joint Acc.	L1 Acc.	L2 Acc.	Acc.
Gemini-3-Pro	<u>40.55</u>	<u>33.79</u>	<u>62.34</u>	<u>33.93</u>	<u>47.31</u>
Qwen3-Omni-30B-A3B	28.00	17.79	64.55	22.76	38.21
Logics-Parsing-Omni	<b>64.69</b>	<b>60.69</b>	<b>82.48</b>	<b>60.69</b>	<b>68.69</b>

Note: Bold text indicates the best result, and underlined text indicates the second-best result.

### Cognition:

- **Avg.:** Represents the overall cognitive capability, calculated as the exact mean of Information Extraction Accuracy and Recognition Accuracy.

$$\text{Avg.} = \frac{1}{2}(\text{Info. Ext.} + \text{Rec.})$$

### Overall:

- **Overall:** Calculated as the unweighted mean of the two primary dimensions, reflecting the model’s comprehensive performance.

$$\text{Overall} = \frac{1}{2}(\text{Perception}_{\text{avg}} + \text{Cognition}_{\text{avg}})$$

## A.4 DETAILED EVALUATION ON THE NATURAL VIDEO MODULE OF OMNIPARSINGBENCH

The exact calculation rules of (Table 7) as follows:

### Perception:

- **Avg.:** Aggregates all video perception metrics, specifically Time F1, Key F1, ASR WER, Visual accuracy, and Camera accuracy.

$$\text{Avg.} = \frac{1}{5}(\text{Time} + \text{Key} + (1 - \min(1, \text{ASR})) \times 100 + \text{Visual} + \text{Camera})$$

### Cognition:

- **Avg.:** Represents the mean accuracy across all cognition sub-categories

$$\text{Avg.} = \frac{1}{8}(\text{Count} + \text{Rec.} + \text{Info. Ext.} + \text{Attr. \& States} + \text{Event} + \text{Camera} + \text{Emot.} + \text{Caus. Rsn.})$$

### Overall:

- **Overall:** Calculated as the unweighted mean of the two primary dimensions, reflecting the model’s comprehensive performance.

$$\text{Overall} = \frac{1}{2}(\text{Perception}_{\text{avg}} + \text{Cognition}_{\text{avg}})$$

Table 18 details the models’ performance on the Camera sub-benchmark. In perception, it attains a joint accuracy of 60.69%, significantly outperforming Gemini-3-Pro and Qwen3-Omni-30B-A3B, especially in fine-grained L2 classification. In semantic cognition, the model reaches 68.69% accuracy (+21% over the strongest baseline), demonstrating superior integration of camera language into

---

multimodal narratives. Overall, it reaches a leading score of 64.69% (calculated as the average of perception joint accuracy and cognition accuracy).

#### A.5 DETAILED EVALUATION ON THE TEXT-RICH VIDEO MODULE OF OMNIPARSINGBENCH

The exact calculation rules of (Table 8) as follows:

##### **Perception:**

- **Avg.:** Aggregates all video perception metrics, specifically Time F1, ASR WER, and Visual OCR Score.

$$\text{Avg.} = \frac{1}{3}(\text{Time} + \text{Visual} + (1 - \min(1, \text{ASR})) \times 100)$$

##### **Cognition:**

- **Avg.:** Represents the mean between the In-Depth Str. Cap. score and the average accuracy of all other Cognition categories.

$$\text{Avg.} = \frac{1}{2}(\text{In-Depth Str. Cap.} + (\frac{1}{7}(\text{Info. Ext.} + \text{Object} + \text{OCR} + \text{Attr. \& States} + \text{Event} + \text{Info. Syn.} + \text{Caus. Rsn.})))$$

##### **Overall:**

- **Overall:** Calculated as the unweighted mean of the two primary dimensions, reflecting the model’s comprehensive performance.

$$\text{Overall} = \frac{1}{2}(\text{Perception}_{\text{avg}} + \text{Cognition}_{\text{avg}})$$

#### A.6 QUALITATIVE DEMONSTRATIONS OF OMNI-MODAL PARSING

In this subsection, we present a comprehensive series of qualitative examples to demonstrate the multifaceted capabilities of Logics-Parsing-Omni. These showcases span our proposed unified taxonomy, encompassing diverse and knowledge-intensive scenarios: from natural image understanding and graphics parsing (e.g., complex charts and geometric illustrations), to multi-image difference reasoning, dynamic audio-visual stream parsing (including natural and text-rich educational videos), and intricate document structural analysis.

Prompt:请检测图中的文本与实体, 提取边界框、标签、属性及详细描述等结构化信息, 并给出全局图像描述。结果以JSON格式输出。

Input Image:



Parsing Visualization:



Logics-Parsing-Omni Parsing Result:

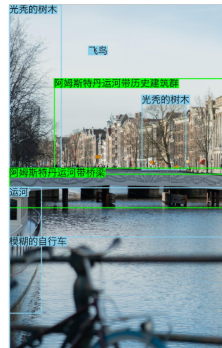
```
[{"category": "entity", "bbox": [357, 0, 532, 147], "tags": {"11": "食物与饮品", "12": "饮品类", "13": "玻璃杯"}, "attributes": {"材质": "玻璃", "内容物颜色": "琥珀色", "形状": "圆柱形", "caption": "一个装有琥珀色液体的玻璃杯, 杯身透明, 液体颜色浓郁, 可能为葡萄酒或烈酒, 杯口部分可见。"}, {"category": "entity", "bbox": [725, 0, 999, 235], "tags": {"11": "食物与饮品", "12": "水果", "13": "一串葡萄"}, "attributes": {"颜色": "深紫色", "表面特征": "有自然光泽", "形态": "成串悬挂", "caption": "一串深紫色的葡萄, 颗粒饱满, 表面有自然光泽, 部分葡萄仍连在藤上, 显得新鲜诱人。"}, {"category": "entity", "bbox": [434, 12, 485, 425], "tags": {"11": "食物与饮品", "12": "蓝纹奶酪", "13": "蓝纹奶酪"}, "attributes": {"形状": "三角形", "颜色": "淡黄色", "纹理特征": "内部有蓝色霉菌", "caption": "一块三角形的蓝纹奶酪, 表面和内部布满蓝色霉菌, 奶酪呈淡黄色, 边缘有部分包装纸残留。"}, {"category": "entity", "bbox": [207, 187, 322, 322], "tags": {"11": "装饰品", "13": "法国国旗小旗"}, "attributes": {"颜色组成": "蓝、白、红三色", "材质": "纸质", "固定方式": "插在牙签上", "caption": "一面插在牙签上的法国国旗小旗, 由蓝、白、红三色竖条组成, 颜色鲜明, 材质为纸质。"}, {"category": "text", "bbox": [187, 300, 322, 380], "tags": {"language": "英文", "label": "拼字游戏瓷砖拼出的英文短语"}, {"category": "entity", "bbox": [0, 697, 322, 999], "tags": {"11": "植物", "12": "花卉", "13": "紫色小花"}, "attributes": {"颜色": "紫色", "形态": "细小簇状", "位置": "画面左下角", "caption": "几朵紫色的小花, 花瓣细小, 枝叶纤细, 散落在布料上, 为画面增添自然气息。"}, {"category": "global", "bbox": [0, 322, 322, 999], "caption": "一块浅色木质砧板斜置于画面中央, 其表面清晰可见天然木纹与轻微的使用痕迹, 边缘略带圆润。砧板上, 由白色方形字母瓷砖拼出的'BASILILLE DAY'字样占据视觉中心, 字母为深绿色, 每个瓷砖右下角标有数字, 如'B'为3, 'A'为1, 'S'为1, 依此类推, 瓷砖排列成两行, 上行'BASILILLE', 下行'DAY'。在字母瓷砖的左上方, 插着一面小巧的法国国旗, 蓝、白、红三色竖条清晰, 旗面固定在一根细长的木签上。字母瓷砖的右上方, 摆放着一块三角形的蓝纹奶酪, 奶酪主体呈淡黄色, 内部与表面散布着不规则的深蓝色霉菌斑点, 其底部仍包裹着部分银色锡箔纸。奶酪的右后方, 是一串饱满的紫黑色葡萄, 果粒圆润, 表面覆有薄薄的白霜, 部分果粒仍连着细小的藤茎。在奶酪后方, 一个深琥珀色的玻璃杯底部边缘可见, 杯中液体颜色与杯身一致。整个砧板置于一块浅灰色的织物之上, 织物表面有细微的纹理。左下角与右下角处, 几枝带有细小紫色花朵的植物枝条自然垂落, 部分枝叶与砧板边缘相接。光线从左上方投射, 在砧板与物体上形成柔和的阴影, 整体色调温暖, 营造出一种静物陈列的氛围。", "tag": "餐饮"}]
```

Prompt:请检测图中的文本与实体, 提取边界框、标签、属性及详细描述等结构化信息, 并给出全局图像描述。结果以JSON格式输出。

Input Image:



Parsing Visualization:



Logics-Parsing-Omni Parsing Result:

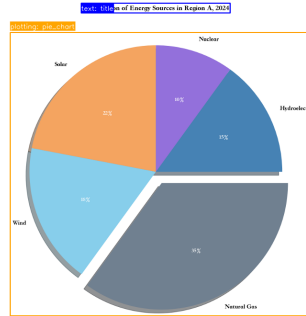
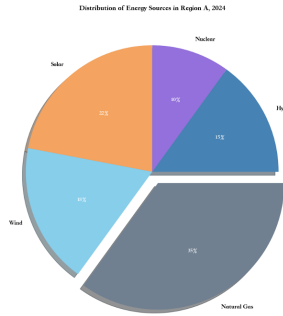
```
[{"category": "entity", "bbox": [0, 0, 228, 485], "tags": {"11": "植物", "12": "乔木与灌木", "label": "光秃的树木"}, "attributes": {"树木状态": "光秃", "枝干形态": "交错", "季节特征": "冬季或早春", "caption": "位于画面左侧的几棵高大落叶树, 枝干光秃, 没有叶子, 显示出冬季或早春的景象。"}, {"category": "entity", "bbox": [344, 120, 385, 128], "tags": {"11": "动物", "12": "野生动物", "label": "飞鸟"}, "attributes": {"飞行状态": "飞翔", "体型特征": "小型", "位置特征": "天空中", "caption": "一只在天空中飞翔的小鸟, 位于画面中上部, 体型较小, 正在空中滑翔。"}, {"category": "entity", "bbox": [385, 207, 485, 808], "tags": {"11": "建筑与设施", "12": "建筑", "label": "大型古典建筑"}, "attributes": {"建筑风格": "古典风格", "立面特征": "立柱和拱形窗户", "屋顶类型": "斜坡屋顶", "caption": "位于画面最右侧的一座宏伟的古典风格建筑, 拥有高大的立柱和精致的立面装饰, 屋顶为斜坡式。"}, {"category": "entity", "bbox": [570, 262, 634, 485], "tags": {"11": "植物", "12": "乔木与灌木", "label": "光秃的树木"}, "attributes": {"树木状态": "光秃", "枝干形态": "交错", "季节特征": "冬季或早春", "caption": "位于画面中右侧的一棵高大落叶树, 枝干光秃, 没有叶子, 显示出冬季或早春的景象。"}, {"category": "entity", "bbox": [634, 190, 698, 808], "tags": {"11": "建筑与设施", "12": "建筑", "label": "一排沿河建筑"}, "attributes": {"建筑风格": "欧洲风格", "外墙颜色": "浅色", "屋顶类型": "斜坡屋顶", "caption": "沿河岸排列的一排多层欧洲风格建筑, 外墙颜色以浅色为主, 屋顶为斜坡式, 部分建筑带有阳台和装饰性山墙。"}, {"category": "entity", "bbox": [698, 120, 739, 808], "tags": {"11": "人物", "12": "群体人物", "label": "人群"}, "attributes": {"人群密度": "密集", "活动状态": "行走或驻足", "位置特征": "桥上", "caption": "站在桥上的一群人, 由于距离较远, 个体细节模糊, 但可以看出他们正在桥上行走或驻足。"}, {"category": "entity", "bbox": [739, 120, 820, 808], "tags": {"11": "建筑与设施", "12": "建筑", "label": "装饰性桥梁"}, "attributes": {"knowledge_tags": {"tag_name": "阿姆斯特丹运河桥", "11": "知名地点与景观", "12": "文化与历史遗迹", "13": "历史建筑与街区"}, "attributes": {"桥梁颜色": "白色", "装饰图案": "灰色抽象图案", "桥墩材质": "深色木质或混凝土", "caption": "一座横跨运河的现代风格桥梁, 桥身呈白色, 带有连续的灰色抽象图案装饰, 桥墩为深色木质结构, 桥上可见行人。该桥是阿姆斯特丹运河网络中典型的桥梁设计, 其独特的装饰图案和结构是该城市水道景观的标志性元素。"}, {"category": "entity", "bbox": [820, 120, 861, 808], "tags": {"11": "人造物体", "12": "交通工具", "label": "游船"}, "attributes": {"船体颜色": "白色", "栏杆颜色": "黑色", "船体形状": "流线型", "caption": "一艘停泊在水边的白色游船, 船体侧面有黑色栏杆, 船头部分可见, 船身呈流线型。"}, {"category": "entity", "bbox": [861, 120, 942, 808], "tags": {"11": "人造物体", "12": "交通工具", "label": "前景中的自行车"}, "attributes": {"颜色": "深色", "清晰度": "模糊", "位置特征": "前景", "caption": "位于画面最前景的一辆自行车, 由于失焦而显得模糊, 只能看到其深色的车架和部分车轮轮廓。"}, {"category": "global", "bbox": [842, 120, 999, 808], "caption": "这张图片展示了一幅典型的阿姆斯特丹运河景观。画面中, 一条宁静的运河蜿蜒穿过城市, 水面平静如镜, 倒映着周围的建筑和树木。运河上横跨着一座装饰有复杂图案的桥梁, 桥身设计精美, 与周围的环境和谐相融。桥下, 几根木桩支撑着桥墩, 显示出历史的痕迹。运河两岸排列着一排排古典建筑, 这些建筑风格统一, 外墙多为浅色, 屋顶呈斜坡状, 带有典型的荷兰建筑特色。建筑物之间点缀着几棵光秃秃的树木, 显示出季节可能是秋冬时节。远处的天空晴朗, 几只飞鸟在空中翱翔, 增添了画面的生动感。在前景中, 一辆自行车的部分轮廓隐约可见, 这是阿姆斯特丹常见的交通工具, 进一步强化了这一场景的地域特色。阿姆斯特丹运河是这座城市的核心景观, 以其160多条运河和1281座桥梁闻名, 建筑风格统一且富有历史感, 自行车文化也十分普及。整张图片完美地捕捉到了阿姆斯特丹运河的独特魅力和宁静氛围。", "tag": "建成区域"}]
```

Figure 9: Qualitative examples illustrating the natural image parsing capability of Logics-Parsing-Omni.

**Prompt:** Perform an in-depth parsing of the image, locate text and charts, extract their bounding boxes, labels, parsing results, and descriptions, and provide a global image description. Please present the results in JSON format.

**Input Image:**

**Output Visualization:**



Energy Source	Percentage
Nuclear	10%
Hydroelectric	15%
Natural Gas	35%
Wind	18%
Solar	22%

**Logics-Parsing-Omni:**

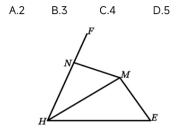
[{"category": "text", "bbox": [271, 14, 712, 43], "tag": "title", "text": "Distribution of Energy Sources in Region A, 2024"}, {"category": "plotting", "bbox": [60, 100, 960, 938], "tag": "pie\_chart", "parsing": "<table><tr><td>Energy Source</td><td>Percentage</td></tr><tr><td>Nuclear</td><td>10%</td></tr><tr><td>Hydroelectric</td><td>15%</td></tr><tr><td>Natural Gas</td><td>35%</td></tr><tr><td>Wind</td><td>18%</td></tr><tr><td>Solar</td><td>22%</td></tr></table>", "caption": "The visualization is a pie chart....(details omitted.)", {"category": "global", "caption": "This is a pie chart titled 'Distribution of Energy Sources in Region A, 2024'. The chart is divided into five colored segments, each representing a different energy source and its percentage share of the total energy distribution for Region A in 2024. The segments are arranged radially around a central point, with labels and percentage values placed adjacent to each segment. The energy sources and their corresponding percentages are: Natural Gas: 35% (represented by a dark gray segment, the largest portion, located at the bottom right). Solar: 22% (represented by an orange segment, located at the top left). Wind: 18% (represented by a light blue segment, located at the bottom left). Hydroelectric: 15% (represented by a medium blue segment, located at the top right). Nuclear: 10% (represented by a purple segment, the smallest portion, located at the top center). The chart visually emphasizes that Natural Gas is the dominant energy source in Region A for 2024, followed by Solar, Wind, Hydroelectric, and Nuclear in descending order of contribution."}]

**Prompt:** 请检测图中的文本和几何形状，提取边界框、标签、解析结果及详细描述，并提供全局图像描述。结果以JSON格式输出。

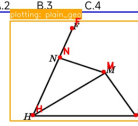
**Input Image:**

**Output Visualization:**

如图，HM是∠FHE的平分线，MN⊥HF于点N，若HE=8.5，∠HEM=12，则MN的长为()



如图，HM是∠FHE的平分线，MN⊥HF于点N，若HE=8.5，∠HEM=12，则MN的长为()



**Logics-Parsing-Omni:**

[{"category": "text", "bbox": [40, 100, 960, 300], "tag": "question", "text": "7. 如图，在△ABC中，∠C=90°，∠ABC=60°，BD平分∠ABC，若BD=6，求AC的长。"}, {"category": "plotting", "bbox": [320, 300, 680, 900], "tag": "plain\_geo", "parsing": [{"Geo\_Elements": [{"points": [{"label": "H", "coord": [370, 870]}, {"label": "E", "coord": [595, 870]}, {"label": "F", "coord": [455, 390]}, {"label": "M", "coord": [525, 630]}, {"label": "N", "coord": [429, 550]}], "lines": [{"line": "HE", "type": "solid"}, {"line": "EF", "type": "solid"}, {"line": "FH", "type": "solid"}, {"line": "HM", "type": "solid"}, {"line": "MN", "type": "solid"}], "arcs": [], "shapes": [{"Shape": "H,E,F"}, {"Shape": "H,M,N"}]}, {"Geo\_Relations": [], "Quantitative\_Relations": []}], "caption": "### \*\*整体概览\*\*\n\n该图是一个由五个主要顶点 (H, E, M, N, F) 和连接它们的直线段构成的平面几何图形。.....(细节省略)。", {"category": "global", "caption": "这是一张包含平面几何图形及其相关文字题目的图像。图像整体布局为左侧是文字题干，右侧是对应的几何图形。"}]

7. 如图，在△ABC中，∠C=90°，∠ABC=60°，BD平分∠ABC，若BD=6，求AC的长。

一、文字题干部分

如图，△ABC中，∠C=90°，∠ABC=60°，BD平分∠ABC，若BD=6，求AC的长。

二、几何图形部分

是一个直角三角形及其内部构造线。

三角形ABC：由三个顶点A、B、C构成。顶点C位于图形的右上角，顶点A位于左下角，顶点B位于右下角。边AC为斜边，边BC为竖直线，边AB为水平底边。在顶点C处，有一个直角符号（小方块），明确标注∠C=90°。在顶点B处，角∠ABC被标注为60°（根据题干文字，图形中未直接标注角度数值，但题干说明）。点D位于边AC上，介于A和C之间。该点被明确标注为大写字母“D”。

线段BD：连接顶点B与边AC上的点D。该线段将∠ABC分为两个角。根据题干，BD是∠ABC的角平分线，因此∠ABD=∠DBC=30°。线段BD的长度在题干中给出为6，即BD=6。

图形结构关系：三角形ABC是一个直角三角形，直角在C。BD是从直角顶点B引出的角平分线，交对边AC于点D。图形中未标注任何长度数值或角度数值，所有数值信息均来自题干文字。

三、整体布局

图像左侧为题干文字，右侧为几何图形，两者并列排布。图形清晰标注了所有顶点(A、B、C、D)和直角符号。所有几何元素均为黑色实线，背景为纯白色。无坐标系、无网格、无其他辅助线或标记。

总结：该图像展示了一个直角三角形ABC(∠C=90°)，其中∠ABC=60°，从顶点B作角平分线BD交AC于D，已知BD=6，要求解边AC的长度。图形与文字共同构成一道完整的平面几何计算题。

Figure 10: Qualitative examples illustrating the graphics image parsing capability of Logics-Parsing-Omni.

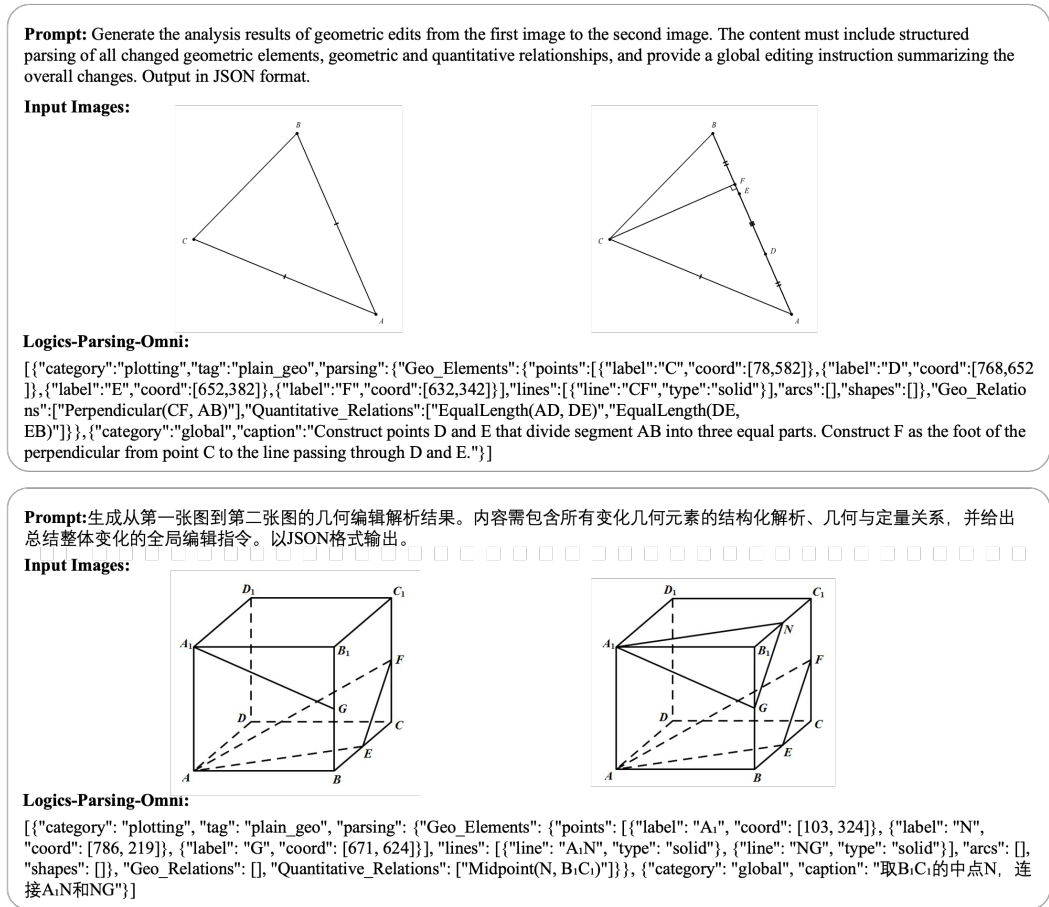


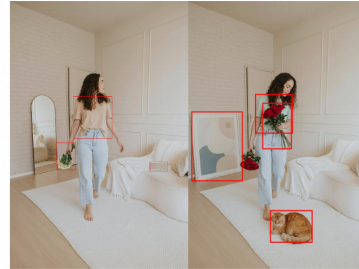
Figure 11: Qualitative examples illustrating the graphics image difference parsing capability of Logics-Parsing-Omni.

**Prompt:** 生成从第一张图编辑到第二张图的结构化解析结果。逐项列出所有变化元素，并给出对应的边界框、标签、属性及描述等信息；最后给出全局编辑描述总结整体变化。以JSON格式输出。

**Input Images:**



**Logics-Parsing-Omni Bbox Visualization:**



**Logics-Parsing-Omni:**

```
[[{"category": "entity", "bbox": [{"source": [355, 357, 573, 513], "target": [374, 347, 587, 495]}, {"tags": [{"1": "人造物体", "2": "服饰与配饰", "3": "T恤"}, {"attributes": {"颜色": "浅绿色"}, {"change_tag": "Modification"}, {"caption": "人物上衣的颜色发生了变化: 在图1中为米色, 在图2中变为浅绿色。"}], {"category": "entity", "bbox": [{"source": [260, 529, 367, 630], "target": [415, 380, 580, 553]}, {"tags": [{"1": "植物", "2": "花卉", "3": "玫瑰"}, {"attributes": {"颜色": "红色", "种类": "玫瑰"}, {"change_tag": "Modification"}, {"caption": "人物手中所持花束的种类和颜色发生了变化: 在图1中为白色小花, 在图2中变为红色玫瑰。"}], {"category": "entity", "bbox": [{"source": null, "target": [458, 781, 697, 902]}, {"tags": [{"1": "动物", "2": "家养动物", "3": "猫"}, {"attributes": {"颜色": "橘色", "姿态": "卧姿", "位置": "地毯上"}, {"change_tag": "Addition"}, {"caption": "一只橘色的猫在图2中被添加到场景中, 它正卧在地毯上, 位于人物的脚边。"}], {"category": "entity", "bbox": [{"source": null, "target": [18, 412, 306, 673]}, {"tags": [{"1": "文化与艺术", "2": "艺术创作", "3": "装饰画"}, {"attributes": {"画框颜色": "白色", "内容": "抽象图案", "位置": "左侧墙边"}, {"change_tag": "Addition"}, {"caption": "一幅带白色画框的抽象画在图2中被添加到场景中, 靠在左侧的墙边。"}], {"category": "entity", "bbox": [{"source": [785, 600, 884, 636], "target": null}, {"tags": [{"1": "人造物体", "2": "电子设备", "3": "笔记本电脑"}, {"attributes": {"颜色": "银色", "位置": "沙发上"}, {"change_tag": "Removal"}, {"caption": "一台银色的笔记本电脑在图1中放置于沙发上, 在图2中被移除。"}], {"category": "global", "caption": "1. 在图1中, 人物手持一束白色小花, 而在图2中, 她手持一束红色玫瑰。2. 在图2中, 人物的上衣颜色从图1的米色变为浅绿色。3. 在图2中, 人物的脚边新增了一只橘色的猫。4. 在图2中, 人物的左侧墙边新增了一幅带白色画框的抽象画。5. 在图1中, 人物的视线朝向右上方, 而在图2中, 她的视线向下看着手中的花束。6. 在图1中, 沙发上的笔记本电脑是打开状态, 而在图2中, 它被移除了。"}], {"tag": "室内场景"}]]
```

Figure 12: Qualitative examples illustrating the natural image difference parsing capability of Logics-Parsing-Omni.



Figure 13: Qualitative examples illustrating the natural video parsing capability of Logics-Parsing-Omni.

**Prompt:** Please analyze the video using OCR information stability as the basis for segmentation, extract the timestamp, OCR, and ASR content of each segment in chronological order, add a global audio-video description at the end, and output the result in JSON format.

**Input Video:**

**Logics-Parsing-Omni:**

```

[{"category": "audio_visual_segment", "timestamp": [0.0, 16.0], "ocr": [{"type": "title", "content": "AN ONLINE LECTURE FOR CHEM 16 GENERAL CHEMISTRY I\n\nSOME PROPERTIES OF THE LIQUID STATE"}, {"type": "text", "content": "PART OF 09 LIQUIDS, SOLIDS, PHASE CHANGES\n\nMedel Manuel L. Zulueta\n\nUPD Institute of Chemistry"}], "asr": ""},
{"category": "audio_visual_segment", "timestamp": [16.0, 141.5], "ocr": [{"type": "title", "content": "The Liquid State: Surface Tension"}, {"type": "text", "content": "\n\nSurface tension: energy required to increase the surface area\n\nThe stronger the forces are between the particles in a liquid, the greater the surface tension\n\nSurfactants (e.g., soaps, emulsifiers) decrease the surface tension of water by congregating at the surface and disrupting the hydrogen bonds\n\nSurface\n\nH-bonding across and beneath the surface; net vector toward the center\n\ninterior\n\nH-bonding occurs in three dimensions"}], "asr": "I will next describe some properties of the liquid state. The first is surface tension. Surface tension is the energy required to increase the surface area of a liquid. In the case of water, hydrogen bonding across and beneath the surface tends to form a net vector towards the center. In the interior of this drop, hydrogen bonding occurs in three dimensions. Thus, the liquid tends to form a spherical shape as the particles within the liquid are attracted towards the center. This form of attraction reduces the surface area of the liquid, and surface tension is the necessary energy to increase this surface area. The stronger the forces are between the particles in a liquid, the greater the surface tension. Surfactants, for example, soaps and emulsifiers, decrease the surface tension of water by congregating at the surface and disrupting the hydrogen bonds. Here are surface tensions of different substances. Mercury, having metallic bonding, has the highest surface tension. Water, which has hydrogen bonding, also exhibits high surface tension. As the energy of attraction between particles decreases, surface tension also decreases."},
{"category": "audio_visual_segment", "timestamp": [141.5, 248.0], "ocr": [{"type": "title", "content": "The Liquid State: Capillarity"}, {"type": "text", "content": "\n\nCapillary action or capillarity\n\nThe rising of a liquid through a narrow space against gravity\n\nAdhesive (H-bonding of water with the glass wall) and cohesive forces (H-bonding within water) raise the water level and produce the concave meniscus, until gravity balances the upward force\n\nThe cohesive forces among the mercury atoms are much stronger than the adhesive forces, producing a convex meniscus\n\nCapillary rise\n\nCapillary fall"}], "asr": "Another property of the liquid state is capillarity. Capillary action or capillarity is the rising of a liquid through a narrow space against gravity. You will often see it when you put a small capillary tube in water. Water tends to rise inside these capillary tubes. This can be explained by two types of forces present. The adhesive force, this is the H bonding of water with a glass wall, and cohesive force, the hydrogen bonding within water, which raises the water level. Together, the adhesive force and cohesive force produce the concave meniscus you often see in these cases, until gravity balances the upward force. The cohesive forces among the mercury atoms are much stronger than the adhesive forces. They produce a convex meniscus. The depression of the liquid level in a convex meniscus is known as capillary fall. The next property of the liquid state is viscosity. Viscosity is the fluid's resistance to flow."},
{"category": "audio_visual_segment", "timestamp": [248.0, 315.0], "ocr": [{"type": "title", "content": "The Liquid State: Viscosity"}, {"type": "text", "content": "\n\nViscosity: a fluid's resistance to flow; results from intermolecular attractions that impede flow\n\nMuch higher in liquid than gases and decrease with heating (e.g., heated oil in a pan)\n\nSmall, spherical molecules have low viscosities and long molecules pour slowly\n\nStronger intermolecular forces create higher viscosity"}], "asr": "This results from intermolecular attractions that impede flow. Viscosity is much higher in liquid than gases and decrease with heating. You will notice this in heating oil in a pan. When you place your oil in a pan, the oil is viscous. But as you heat it up, the viscosity of the oil decreases. Small spherical molecules have low viscosities and long molecules pour slowly. Stronger intermolecular forces create higher viscosity. Water is a great solvent due to its polarity and exceptional hydrogen bonding ability."},
{"category": "audio_visual_segment", "timestamp": [315.0, 381.5], "ocr": [{"type": "title", "content": "Unique Properties of Water"}, {"type": "text", "content": "\n\nGreat solvent properties due to polarity and exceptional H-bonding ability\n\nExceptionally high specific heat capacity and high heat of vaporization\n\nGive Earth and its organisms a narrow temperature range\n\nHigh surface tension and capillarity\n\nThe solid state has lower density than the liquid state"}], "asr": "It has exceptionally high specific heat capacity and high heat of vaporization. This gives Earth and its organisms a narrow temperature range. Water has high surface tension and capillarity. And the solid state has lower density than the liquid state. This is very useful in frozen lakes, where the ice is on top, and the bottom, which remains liquid, prevents aquatic life from freezing."},
{"category": "global", "caption": "This educational video presents a lecture on the physical properties of liquids, part of a General Chemistry I course. The presentation begins with a title slide introducing the topic: 'Some Properties of the Liquid State,' delivered by Medel Manuel L. Zulueta of the UPD Institute of Chemistry. The lecture opens with surface tension, defined as the energy required to increase a liquid's surface area. A visual of a water droplet appears, illustrating how hydrogen bonding at the surface creates a net inward force, while molecules in the interior experience balanced, three-dimensional attractions. This imbalance causes liquids to minimize surface area, forming spheres. The video explains that stronger intermolecular forces correlate with higher surface tension and notes that surfactants like soap reduce water's surface tension by disrupting hydrogen bonds at the surface. A table compares surface tension values at 20°C for various substances, highlighting mercury's exceptionally high value due to metallic bonding, followed by water's high value from hydrogen bonding, and lower values for substances with weaker intermolecular forces like diethyl ether. Next, the video transitions to capillarity—the ability of a liquid to rise in a narrow tube against gravity. A diagram shows water rising in a glass capillary tube, forming a concave meniscus. This behavior is explained by the interplay of adhesive forces (water molecules bonding to the glass) and cohesive forces (water molecules attracting each other via hydrogen bonding). The upward pull from adhesion and cohesion is balanced by gravity, resulting in a stable liquid height. In contrast, mercury in a glass tube forms a convex meniscus because its strong cohesive forces overpower the weaker adhesive forces between mercury and glass, causing the liquid to depress and demonstrating capillary fall. The lecture then addresses viscosity, defined as a fluid's resistance to flow, which arises from intermolecular attractions. Visuals of honey being poured and water flowing from a tap illustrate the concept. The video notes that liquids generally have much higher viscosity than gases and that viscosity decreases with heating—demonstrated by the example of oil becoming less viscous when heated in a pan. Molecular size and shape also influence viscosity: small, spherical molecules flow easily, while long-chain molecules pour more slowly. Stronger intermolecular forces result in higher viscosity. Finally, the video summarizes the unique properties of water. A molecular model of water appears alongside text highlighting its polarity and exceptional hydrogen bonding, which make it an excellent solvent. Water's high specific heat capacity and high heat of vaporization help regulate Earth's temperature and stabilize environments for life. Its high surface tension and capillarity are essential for biological processes like water transport in plants. Crucially, the video notes that ice is less dense than liquid water—a rare property that allows ice to float, insulating aquatic ecosystems and preventing lakes from freezing solid. This density anomaly is visually reinforced with a molecular diagram showing the open, hexagonal structure of ice compared to the more compact arrangement of liquid water molecules."}]

```

Figure 14: Qualitative example illustrating the comprehensive text-rich video parsing capability of Logics-Parsing-Omni.

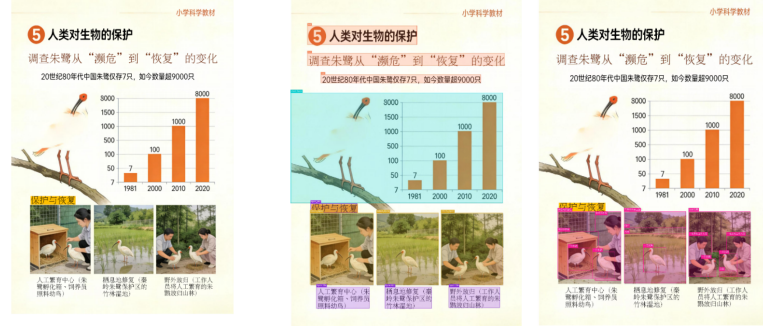




Figure 16: Qualitative example illustrating the comprehensive document structure and semantic parsing capability of Logics-Parsing-Omni on the geometric illustration.

**Prompt:** Output the parsing results of this document in JSON format. Include descriptions for illustrations, structurally parse natural images and graphics, and add a global overview at the end. Use the same language as the the document text.

**Input Image:**



Year	Value
1981	7
2000	100
2010	1000
2020	8000

**Logics-Parsing-Omni:**

[{"category": "text", "bbox": [72, 79, 546, 137], "text": "5 人类对生物的保护", "category": "text", "bbox": [72, 163, 201, 211], "text": "调查朱鹭从“濒危”到“恢复”的变化", "category": "text", "bbox": [72, 211, 201, 221], "text": "20世纪80年代中国朱鹭仅存7只，如今数量超9000只"}, {"category": "text", "bbox": [72, 221, 201, 231], "text": "8000"}, {"category": "text", "bbox": [72, 231, 201, 241], "text": "1500"}, {"category": "text", "bbox": [72, 241, 201, 251], "text": "100"}, {"category": "text", "bbox": [72, 251, 201, 261], "text": "7"}, {"category": "text", "bbox": [72, 261, 201, 271], "text": "1981"}, {"category": "text", "bbox": [72, 271, 201, 281], "text": "2000"}, {"category": "text", "bbox": [72, 281, 201, 291], "text": "2010"}, {"category": "text", "bbox": [72, 291, 201, 301], "text": "2020"}, {"category": "text", "bbox": [72, 301, 201, 311], "text": "1981"}, {"category": "text", "bbox": [72, 311, 201, 321], "text": "2000"}, {"category": "text", "bbox": [72, 321, 201, 331], "text": "2010"}, {"category": "text", "bbox": [72, 331, 201, 341], "text": "2020"}, {"category": "text", "bbox": [72, 341, 201, 351], "text": "1981"}, {"category": "text", "bbox": [72, 351, 201, 361], "text": "2000"}, {"category": "text", "bbox": [72, 361, 201, 371], "text": "2010"}, {"category": "text", "bbox": [72, 371, 201, 381], "text": "2020"}, {"category": "text", "bbox": [72, 381, 201, 391], "text": "1981"}, {"category": "text", "bbox": [72, 391, 201, 401], "text": "2000"}, {"category": "text", "bbox": [72, 401, 201, 411], "text": "2010"}, {"category": "text", "bbox": [72, 411, 201, 421], "text": "2020"}, {"category": "text", "bbox": [72, 421, 201, 431], "text": "1981"}, {"category": "text", "bbox": [72, 431, 201, 441], "text": "2000"}, {"category": "text", "bbox": [72, 441, 201, 451], "text": "2010"}, {"category": "text", "bbox": [72, 451, 201, 461], "text": "2020"}, {"category": "text", "bbox": [72, 461, 201, 471], "text": "1981"}, {"category": "text", "bbox": [72, 471, 201, 481], "text": "2000"}, {"category": "text", "bbox": [72, 481, 201, 491], "text": "2010"}, {"category": "text", "bbox": [72, 491, 201, 501], "text": "2020"}, {"category": "text", "bbox": [72, 501, 201, 511], "text": "1981"}, {"category": "text", "bbox": [72, 511, 201, 521], "text": "2000"}, {"category": "text", "bbox": [72, 521, 201, 531], "text": "2010"}, {"category": "text", "bbox": [72, 531, 201, 541], "text": "2020"}, {"category": "text", "bbox": [72, 541, 201, 551], "text": "1981"}, {"category": "text", "bbox": [72, 551, 201, 561], "text": "2000"}, {"category": "text", "bbox": [72, 561, 201, 571], "text": "2010"}, {"category": "text", "bbox": [72, 571, 201, 581], "text": "2020"}, {"category": "text", "bbox": [72, 581, 201, 591], "text": "1981"}, {"category": "text", "bbox": [72, 591, 201, 601], "text": "2000"}, {"category": "text", "bbox": [72, 601, 201, 611], "text": "2010"}, {"category": "text", "bbox": [72, 611, 201, 621], "text": "2020"}, {"category": "text", "bbox": [72, 621, 201, 631], "text": "1981"}, {"category": "text", "bbox": [72, 631, 201, 641], "text": "2000"}, {"category": "text", "bbox": [72, 641, 201, 651], "text": "2010"}, {"category": "text", "bbox": [72, 651, 201, 661], "text": "2020"}, {"category": "text", "bbox": [72, 661, 201, 671], "text": "1981"}, {"category": "text", "bbox": [72, 671, 201, 681], "text": "2000"}, {"category": "text", "bbox": [72, 681, 201, 691], "text": "2010"}, {"category": "text", "bbox": [72, 691, 201, 701], "text": "2020"}, {"category": "text", "bbox": [72, 701, 201, 711], "text": "1981"}, {"category": "text", "bbox": [72, 711, 201, 721], "text": "2000"}, {"category": "text", "bbox": [72, 721, 201, 731], "text": "2010"}, {"category": "text", "bbox": [72, 731, 201, 741], "text": "2020"}, {"category": "text", "bbox": [72, 741, 201, 751], "text": "1981"}, {"category": "text", "bbox": [72, 751, 201, 761], "text": "2000"}, {"category": "text", "bbox": [72, 761, 201, 771], "text": "2010"}, {"category": "text", "bbox": [72, 771, 201, 781], "text": "2020"}, {"category": "text", "bbox": [72, 781, 201, 791], "text": "1981"}, {"category": "text", "bbox": [72, 791, 201, 801], "text": "2000"}, {"category": "text", "bbox": [72, 801, 201, 811], "text": "2010"}, {"category": "text", "bbox": [72, 811, 201, 821], "text": "2020"}, {"category": "text", "bbox": [72, 821, 201, 831], "text": "1981"}, {"category": "text", "bbox": [72, 831, 201, 841], "text": "2000"}, {"category": "text", "bbox": [72, 841, 201, 851], "text": "2010"}, {"category": "text", "bbox": [72, 851, 201, 861], "text": "2020"}, {"category": "text", "bbox": [72, 861, 201, 871], "text": "1981"}, {"category": "text", "bbox": [72, 871, 201, 881], "text": "2000"}, {"category": "text", "bbox": [72, 881, 201, 891], "text": "2010"}, {"category": "text", "bbox": [72, 891, 201, 901], "text": "2020"}, {"category": "text", "bbox": [72, 901, 201, 911], "text": "1981"}, {"category": "text", "bbox": [72, 911, 201, 921], "text": "2000"}, {"category": "text", "bbox": [72, 921, 201, 931], "text": "2010"}, {"category": "text", "bbox": [72, 931, 201, 941], "text": "2020"}, {"category": "text", "bbox": [72, 941, 201, 951], "text": "1981"}, {"category": "text", "bbox": [72, 951, 201, 961], "text": "2000"}, {"category": "text", "bbox": [72, 961, 201, 971], "text": "2010"}, {"category": "text", "bbox": [72, 971, 201, 981], "text": "2020"}, {"category": "text", "bbox": [72, 981, 201, 991], "text": "1981"}, {"category": "text", "bbox": [72, 991, 201, 1000], "text": "2000"}, {"category": "text", "bbox": [72, 1000, 201, 1000], "text": "2010"}, {"category": "text", "bbox": [72, 1000, 201, 1000], "text": "2020"}]

Figure 17: Qualitative example illustrating the comprehensive document structure and semantic parsing capability of Logics-Parsing-Omni on the graphics and natural illustrations.